Tectonics

RESEARCH ARTICLE
10.1029/2020TC006561

Key Points:

- Sediment sources for the Kootenai Formation were Jurassic continental strata, lower-middle Paleozoic strata, and Jurassic hinterland plutons
- Sediment was delivered to the foreland by transverse fluvial systems from the west and axial systems from the south
- Provenance in the foreland provides insight into the terrane translation history in the hinterland of the orogen

Supporting Information:

Supporting Information may be found in the online version of this article.

Correspondence to:

J. A. Rosenblume,
justin-rosenblume@uiowa.edu

Citation:

Rosenblume, J. A., Finzel, E. S., & Pearson, D. M. (2021). Early Cretaceous provenance, sediment dispersal, and foreland basin development in southwestern Montana, North American Cordillera. *Tectonics*, *40*, e2020TC006561. https://doi.org/10.1029/2020TC006561

Received 7 OCT 2020
Accepted 2 MAR 2021

Early Cretaceous Provenance, Sediment Dispersal, and Foreland Basin Development in Southwestern Montana, North American Cordillera

Justin A. Rosenblume[1], Emily S. Finzel[1], and David M. Pearson[2]

[1]Earth and Environmental Sciences Department, University of Iowa, Iowa City, IA, USA, [2]Department of Geosciences, Idaho State University, Pocatello, ID, USA

Abstract The Lower Cretaceous Kootenai Formation in western Montana records the onset of foredeep sedimentation in the Idaho-Montana retroforeland basin of the North American Cordillera. Contrasting models for sediment dispersal during Early Cretaceous time have been proposed. We use sandstone petrography, large-*n* ($n = 600$) detrital zircon U-Pb geochronology, and mixture modeling to determine the provenance of the Kootenai Formation. These new data combined with additional data from the literature suggest three discrete provenance signatures. Type I sandstones are quartz-rich with U-Pb age peaks at ca. 158, 238, 410, 600, and 1,035 Ma; they were sourced from exhumed Jurassic continental strata and transported northward by axial drainages. Type II sandstones are lithic-rich with U-Pb age peaks at ca. 154, 166, 1,840, 1,920, 2,080, and 2,700 Ma; they were deposited by transverse rivers that drained exhumed lower-middle Paleozoic strata from the Sevier belt. Type III sandstones contain feldspars and minor volcanic lithics with U-Pb age spectra that are dominated by ca. 112 and 162 Ma ages; they were transported by transverse drainages that connected the hinterland of the orogen with the western Montana foreland. Based on provenance analysis of the Kootenai Formation, subtle Early Cretaceous thick-skinned deformation in southwestern Montana did not exhume basement nor did it partition the foreland into locally sourced depocenters. Sediment sources for the western Montana foreland are consistent with those to the north in Alberta and different than southern Idaho. These data also provide insight into the translational history of terranes in the hinterland of the orogen during this time.

1. Introduction

Retroforeland basins form adjacent to fold-thrust belts and contain the stratigraphic record of mountain building (DeCelles, 2012; Ingersoll, 2012). In some cases, where portions of the hinterland have been displaced along major strike-slip faults, the foreland basin system may hold key information for unraveling complex geological histories as it remained stationary on the continent during orogenesis (e.g., Wyld et al., 2006). During Early Cretaceous time, the western margin of the Idaho-Montana sector of the North America Cordillera was subject to outboard terrane accretion and translation, decreased arc magmatism, growth of the Sevier orogenic belt, and development of a retroforeland basin system on the stable portion of the continent (Figure 1; DeCelles, 2004; Gehrels et al., 2009; Gray et al., 2019; Wyld et al., 2006). During this time, this foreland basin system expanded to several hundred kilometers in width, developed an asymmetric geometry, and spanned the length of the continent (DeCelles, 2004).

Numerous models for North American sediment dispersal during Early Cretaceous time have been proposed. However, there is a notable gap in U-Pb detrital zircon data from the Idaho-Montana sector of the foreland basin system (e.g., Blum & Pecha, 2014; Leier & Gehrels, 2011; Schwartz & DeCelles, 1988). Some regional models for this time interval have focused on complexity in southwestern Montana, where early activity along thick-skinned thrusts has been documented in the distal parts of the foreland; these prior studies suggest that the record of basement-involved deformation may substantially predate activity along similar thick-skinned structures elsewhere in the Laramide province (Carrapa et al., 2019; DeCelles, 1986; Schwartz & DeCelles, 1988). In contrast, other models have interpreted sediment dispersal on a continental—rather than regional—scale (e.g., Benyon et al., 2016; Blum & Pecha, 2014; Leier & Gehrels, 2011; Raines et al., 2013). The addition of our new U-Pb detrital zircon provenance data from the southwestern

10.1029/2020TC006561

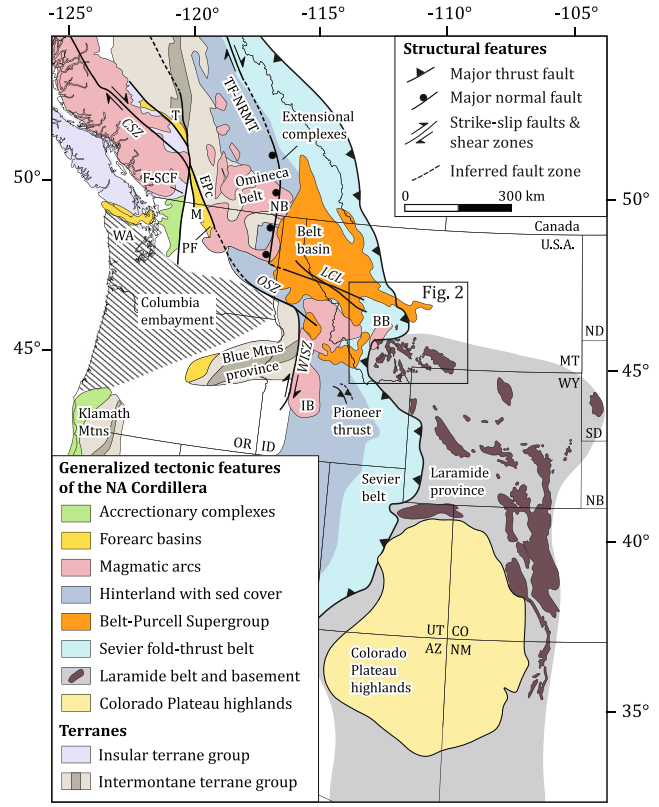

Figure 1. Generalized tectonic map of the North American Cordillera in the western United States and southern Canada (coordinates displayed as NAD83; map features adapted from: Beranek et al., 2016—Pioneer thrust; Brown & Gehrels, 2007—accretionary complex in Washington; Carrapa et al., 2019—thrust front; Dickinson & Gehrels, 2009a—Colorado Plateau highlands; Foster et al., 2006—exposed basement; Gehrels et al., 2009—Coast Mountains batholith; McClelland et al., 1992—faults and forearc basins; McClelland & Oldow, 2007—WISZ, OSZ, batholiths in Omineca belt; Surpless et al., 2014—faults and forearc basins; van der Velon & Cook, 1996—TF-NRMT and extensional complexes; Whitmeyer & Karlstrom, 2007—Belt basin; Wyld et al., 2006—Columbia embayment; Yonkee & Weil, 2015—generalized tectonic domains). Map feature abbreviations: Boulder batholith (BB), Coast shear zone (CSZ), Eagle Plutonic Complex (EPc), Fraser-Straight Creek Fault (F-SCF), Idaho batholith (IB), Lewis and Clark line (LCL), Methow basin (M), Nelson batholith (NB), Orofino shear zone (OSZ), Pasayten Fault (PF), Tyaughton basin (T), Tintina Fault and Northern Rocky Mountain Trench (TF-NRMT), western Idaho shear zone (WISZ).

Montana foreland (Figure 2) allows for refinement of regional sediment dispersal models within the broader context of continental-scale sediment dispersal systems.

In this study, we aim to critically evaluate previous tectonic models by filling the gap in provenance data for the Idaho-Montana sector of the foreland basin system. To achieve this goal, we use sandstone petrography, large-*n* detrital zircon U-Pb geochronology, provenance mixture modeling, and statistical comparisons of detrital age spectra. Our new data provide a better understanding of the provenance and associated sediment dispersal patterns during Early Cretaceous time, especially when integrated with existing petrographic and detrital geochronologic data. Based on our provenance analysis, we infer that Lower Cretaceous sediments were delivered to the western Montana foreland by a combination of transverse and axial drainages from mainly extrabasinal sources. These new data also suggest that the exhumation levels in the fold-thrust belt were similar from Idaho-Montana through southern Canada. Lastly, our provenance interpretations establish potential linkages between the foreland basin system and outboard terranes.

2. Background

2.1. Tectonic Setting and Regional Structure

The North American Cordillera is an accretionary ocean-continent orogenic system that formed during Jurassic to early Cenozoic subduction of oceanic lithosphere beneath western North America (e.g., Dickinson, 2004). Convergence during this time resulted in closure of marginal ocean basins and accretion of fringing arc assemblages, which developed into a collage of terranes along the western margin of North America (Coney & Evenchick, 1994; Monger et al., 1982). Sinistral displacement of these terranes during Early and middle Cretaceous time (e.g., Chardon et al., 1999; Enkin, 2006; Gehrels et al., 2009) was followed by dextral translation during middle Cretaceous to early Cenozoic time; the magnitude of translation remains debated (e.g., Enkin, 2006; Wyld et al., 2006). At the current latitude of the Idaho-Montana region (Figure 1), the dextral transpressive western Idaho shear zone represents a major margin-parallel structure that was active during middle Cretaceous time (e.g., McClelland et al., 2000). Estimates of translation along this structure are ~15–90 km (Giorgis et al., 2005, 2008), ~400 km (Gaschnig et al., 2017; LaMaskin et al., 2011), and >1,000 km (Housen & Dorsey, 2005); most workers agree that major translation (>1,000 km) cannot exclusively rely on this structure (e.g., Gaschnig et al., 2017; Giorgis et al., 2008; Lund & Snee, 1988; McClelland et al., 2000; Wyld et al., 2006).

Differing tectonic reconstructions have been presented for the outboard region of the Idaho-Montana sector of the orogen during Early Cretaceous time. In the modern configuration, the Blue Mountains province in Oregon is juxtaposed with western Idaho and the western Idaho shear zone is cross-cut by or continuous with the Orofino shear zone (Figure 1; Dorsey & LaMaskin, 2007, Giorgis et al., 2008; LaMaskin et al., 2011; McClelland & Oldow, 2007; McClelland et al., 2000; Schmidt et al., 2017). Some workers have suggested that terranes with island arc affinities, presently located in British Columbia, may have been translated northward along the western Idaho shear zone during middle to Late Cretaceous time (e.g., Giorgis et al., 2008; Wyld et al., 2006). One tectonic reconstruction places the Blue Mountains province very near to its modern day position in northeastern Oregon around ~112 Ma (Gray et al., 2019). In contrast, other workers have interpreted that the Blue Mountains province may have been as far south as western Nevada around ~110 Ma, allowing for the possibility that other outboard terranes may have occupied the Oregon-Idaho region during

10.1029/2020TC006561

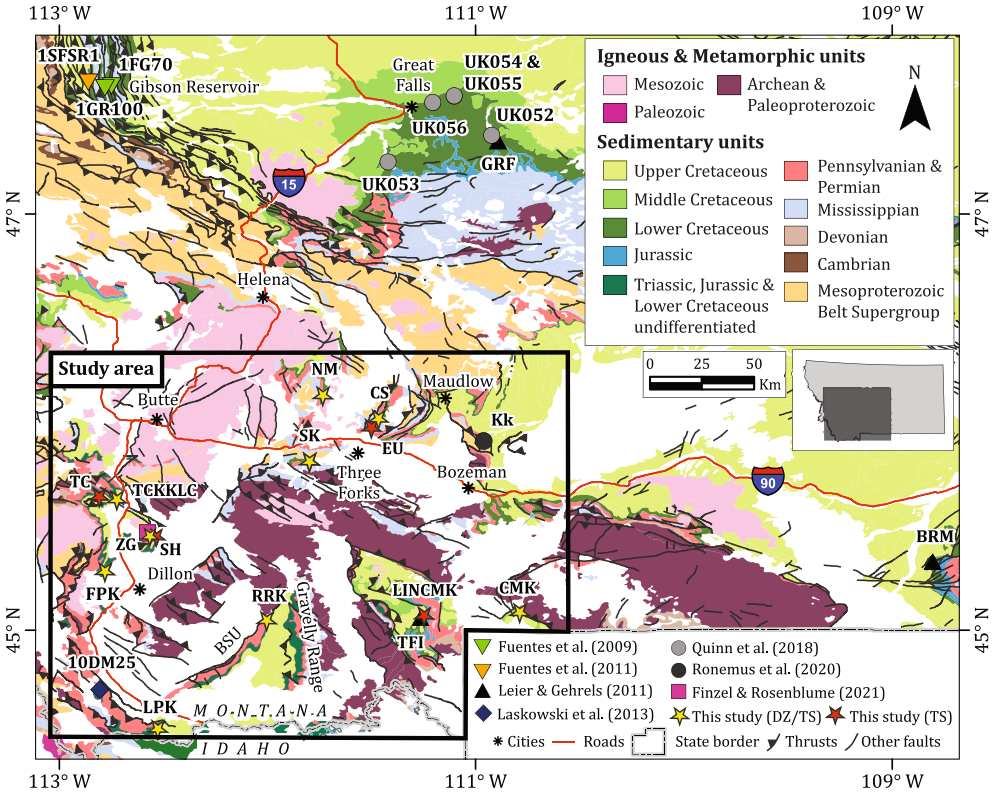

Figure 2. Geologic map of Montana displaying Lower Cretaceous Kootenai Formation sample localities from this study and previously published localities of interest (after Vuke et al., 2007). Map projection is planar and coordinates are displayed as NAD83. Refer to Table 1 and Supporting Information for sample locality descriptions; BSU—Blacktail-Snowcrest uplift; DZ/TS—detrital zircon and thin section sample; TS—thin section sample only.

Early Cretaceous time (Dorsey & LaMaskin, 2007; Gaschnig et al., 2017; Wernicke & Klepacki, 1988; Wyld et al., 2006).

Inboard of the hinterland, the Idaho-Montana sector of the fold-thrust belt contains overlap between thick-skinned and thin-skinned contractional structures (Schmidt & Garihan, 1983; Schmidt & O'Neill, 1983; Schmidt et al., 1988). This region marks the northernmost extent of basement-involved tectonism that constitutes the structurally defined Laramide province (Dickinson & Snyder, 1978). However, most deformation associated with Laramide-age tectonism occurred during Late Cretaceous to Early Cenozoic time (e.g., Copeland et al., 2017). Deformation in the central Idaho portion of the fold-thrust belt was mainly accommodated by folding and thin-skinned thrusting along the Pioneer and subsidiary thrusts (Figure 1) that deformed Neoproterozoic and younger passive margin strata (Brennan et al., 2020; Dover, 1980; Montoya, 2019; Rodgers et al., 1995; Skipp & Hait, 1977). Additionally, exhumed Mesoproterozoic rift-related strata from the Belt-Purcell Supergroup (Figure 1) were also incorporated into the thrust belt in this region (Price, 1981; Ryder & Scholten, 1973). The timing of Early Cretaceous thrusting is poorly constrained. However, plutons that cross-cut the Pioneer thrust sheet indicate that thrusting ceased prior to ~97 Ma (Montoya, 2019). Continued shortening during middle Cretaceous through early Cenozoic time was accommodated by thin- and thick-skinned thrusting in east-central Idaho and southwestern Montana (Garber et al., 2020; Lonn et al., 2016; Perry et al., 1983; Ruppel & Lopez, 1984; Schmidt et al., 1988; Skipp, 1988; Tysdal, 2002).

2.2. Retroforeland Basin System

Retroforeland basins are generally characterized by four discrete depozones (wedge-top, foredeep, forebulge, and backbulge) that occur between the fold-thrust belt and the stable portion of a craton (DeCelles, 2012;

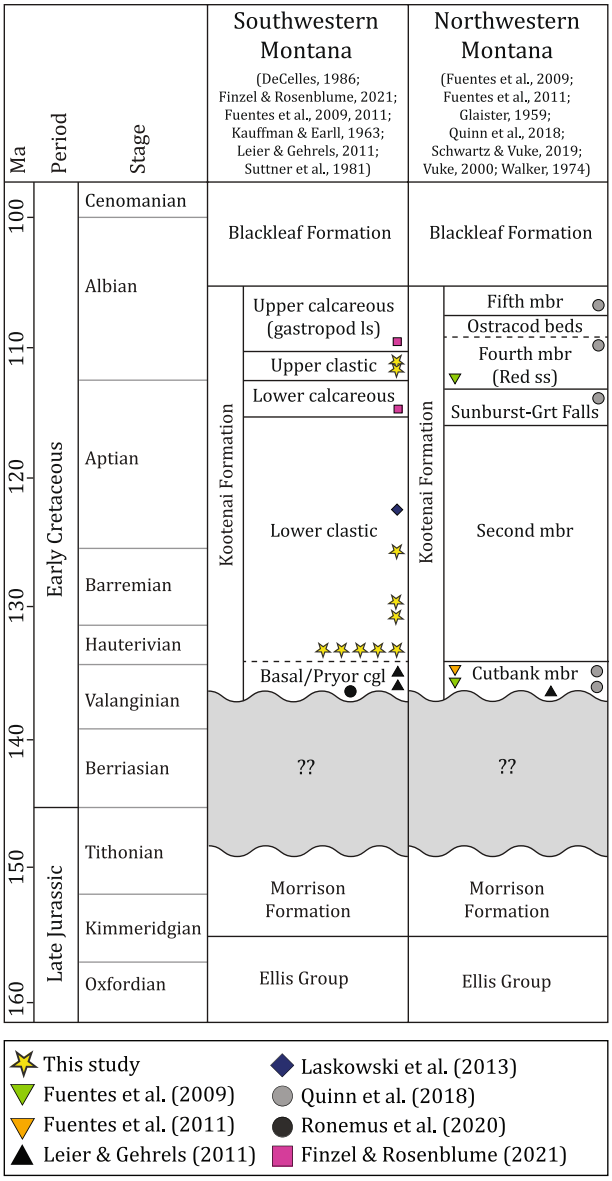

Figure 3. Stratigraphic columns of Late Jurassic and Early Cretaceous strata from southwestern and northwestern Montana with focus on the Kootenai Formation (modified from Raines et al., 2013). Samples are organized by maximum depositional age. Precise absolute age of the lowermost Kootenai Formation remains undetermined; however, it may be as young as Aptian.

DeCelles & Giles, 1996). During Jurassic through early Cenozoic time, a prominent north-south trending retroforeland basin system developed on the North American continent; little doubt remains that the system was consolidated along the entire margin by Early Cretaceous time (DeCelles, 2004; Gillespie & Heller, 1995; Miall, 2009; Yonkee & Weil, 2015). Most workers agree that Lower Cretaceous strata from northern Montana to southern Utah were deposited in the foredeep depozone; this interpretation stems from a general westward thickening of strata, flexural modeling, and subsidence history analysis (DeCelles, 2004; Heller et al., 1986; Jordan, 1981; Suttner et al., 1981). Proximal foredeep strata in southeastern Idaho consist of a >1 km-thick succession referred to as the Gannett Group, which contains numerous conglomerate beds (DeCelles et al., 1993; Gentry et al., 2018). In contrast, in western Montana, Lower Cretaceous strata (Figure 3) are interpreted as distal foredeep deposits on the basis of their much lower sediment thickness (<400 m), the presence of a thin (<5 m) pebble-cobble lag near the base of the succession, and broad regions of lacustrine carbonate deposition (DeCelles, 1986; Fuentes et al., 2011; Holm et al., 1977; Suttner et al., 1981; Zaleha, 2006). Based on these differences, the proximal portions of the foredeep in western Montana are thought to have been entirely eroded from older sedimentary units in the Idaho-Montana region, resulting in a missing or phantom foredeep as has been documented in west-central Utah (Fuentes et al., 2011; Royse, 1993).

2.3. Early Cretaceous Sediment Dispersal

Paleogeographic reconstructions and previous provenance work suggest an Early Cretaceous North American sediment dispersal system that includes western- and eastern-sourced drainages, both of which transported sediment toward a paleo-shoreline in northern Alberta and British Columbia, Canada (Benyon et al., 2014, 2016; Blum & Pecha, 2014; Laskowski et al., 2013; Leier & Gehrels, 2011; May et al., 2013; Quinn et al., 2018; Raines et al., 2013). During this time, these drainages fed three main paleovalley systems in western Canada, which effectively routed sediments to the north-northwest (Horner et al., 2019; Leckie & Smith, 1992). Most workers have interpreted a continental drainage divide in the Montana region based on a difference in detrital zircon provenance signatures; one signature is restricted to near the thrust belt and the other is more widespread to the east (e.g., Leier & Gehrels, 2011). Paleocurrent indicators in the Montana region suggest mainly east- and north-flowing systems (DeCelles, 2004; Heller & Paola, 1989; Hopkins, 1985; Quinn et al., 2018; Walker, 1974); however, in portions of southwestern Montana river systems may have meandered in complex patterns prior to heading north (e.g., DeCelles, 1986).

2.4. Kootenai Formation

The Lower Cretaceous Kootenai Formation in southwestern Montana (Figures 3 and 4) records the onset of foredeep sedimentation. Isopach maps illustrate its asymmetric geometry: The westernmost preserved portions are <400 m thick and the formation thins eastward toward central Montana where it is just 10s of meters thick (Figure 4; Berg et al., 1999; DeCelles, 2004; Fuentes et al., 2011; Schwartz, 1983; Suttner et al., 1981; Walker, 1974). The base of the Kootenai Formation rests on a sub-Cretaceous unconformity, an erosional surface between Late Jurassic and Early Cretaceous strata that represents an ~20 Myr hiatus (Gillespie, 1992; Fuentes et al., 2011). In southwestern Montana, the surface is mainly disconformable

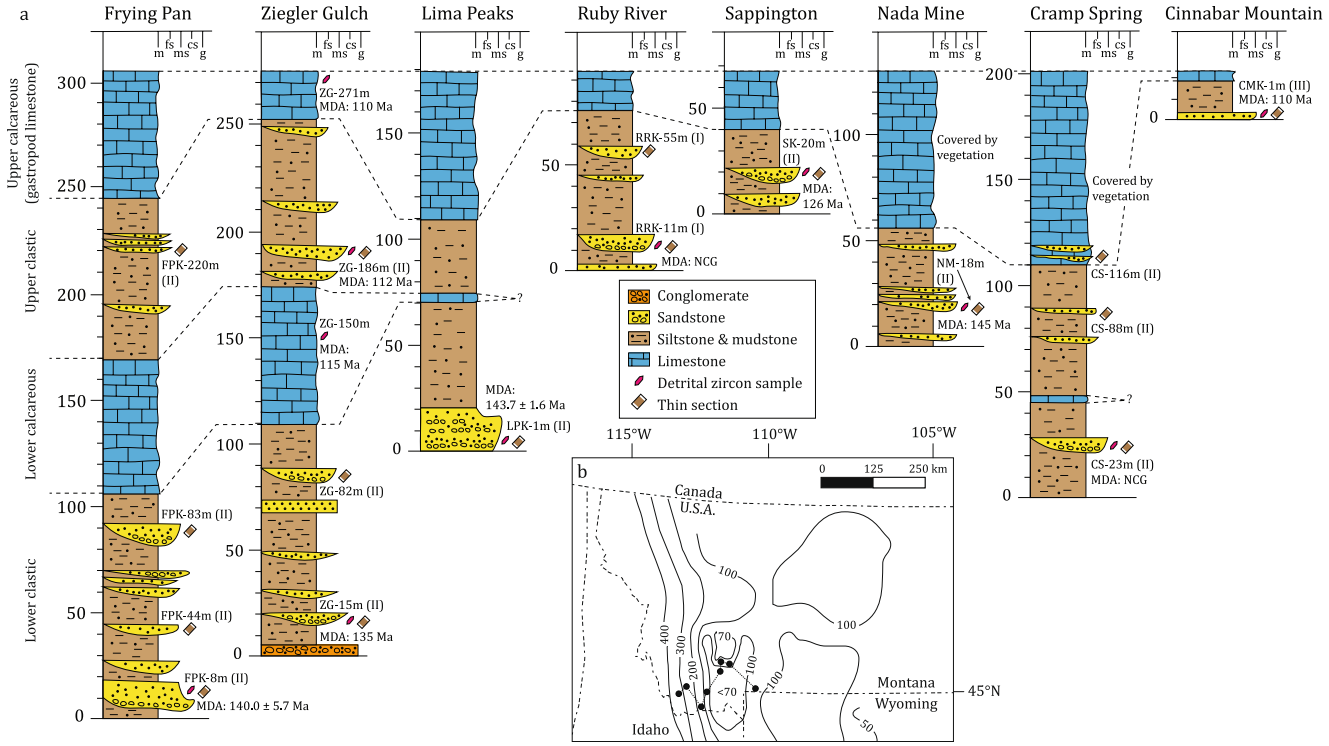

Figure 4. (a) Measured sections of the Kootenai Formation in southwestern Montana correlated from west to east through the study area. The top of the gastropod limestone is taken as a regional datum for this stratigraphic cross-section. Sampled intervals, sandstone types (described in the text), and maximum depositional ages (MDAs) are listed next to each column for context; NCG = no Cretaceous grains. (b) Palinspastic isopach map of Lower Cretaceous strata contoured in meters (after DeCelles, 2004). Black dots represent the approximate localities of measured sections.

with low relief where the Kootenai Formation rests atop the Jurassic Morrison Formation (Gillespie, 1992; Mudge, 1972). Locally, angular unconformities have been recognized between the Jurassic Morrison and Cretaceous Kootenai formations in only two locations in the study area: one near Maudlow, MT and the other near the Gravelly Range (Figure 2; DeCelles, 1986; Mann, 1954; Walker, 1974). The top of the Kootenai Formation is generally gradational with the overlying Blackleaf Formation in the western portion of the study area (James, 1977; Schwartz, 1972), but some workers have documented a disconformable contact between the two units in the eastern portion of the study area (Roberts, 1972; Schwartz, 1972; Vuke, 1982).

Sedimentological studies suggest that the Kootenai Formation in western Montana represents a dominantly nonmarine depositional system that was only locally connected to the Boreal Sea in northern Montana as it encroached southward from Canada (DeCelles, 1986; James, 1980; Schwartz, 1972; Schwartz & Vuke, 2019; Suttner et al., 1981; Vuke, 1984; Walker, 1974). Throughout much of western Montana, the formation is entirely nonmarine with the exception of the Sunburst-Great Falls Member in north-central Montana (Reid, 2015; Schwartz & Vuke, 2019; Walker, 1974). However, there are notable differences within the formation between southwestern and northwestern Montana. For example, four informal members are recognized in the south, whereas five occur in the north (Figure 3; Glaister, 1959; Gwinn, 1965; Kauffman & Earll, 1963; Schwartz & Vuke, 2019; Suttner, 1969; Vuke, 2000; Walker, 1974). Throughout much of western Montana, the Kootenai Formation is composed of fluvial conglomerate, sandstone, siltstone, mudstone, and lacustrine limestone, however, a key difference is that local volcaniclastic sandstones in the upper part of the formation are much more prevalent in the north (Cobban, 1955; DeCelles, 1986; Fuentes et al., 2011; Gillespie, 1992; Quinn et al., 2018; Suttner, 1969).

In southwestern Montana, the Kootenai Formation consists of four informal members: the Lower clastic, Lower calcareous, Upper clastic, and Upper calcareous or gastropod limestone (Figure 3). The Lower calcareous member pinches out to the east (Figure 4). One depositional model interprets that the clastic members were deposited by fluvial systems during pulses of tectonism whereas the calcareous members, which were

deposited in lacustrine systems, represent tectonic quiescence (DeCelles, 1986; Schwartz, 1983; Schwartz & DeCelles, 1988). In that model, heterogeneity in the thickness of sandstones within the Lower clastic member was used to infer tectonic partitioning into distinct subbasins during early growth of low-magnitude, intraforeland basement arches, and doming above igneous intrusive rocks. However, geochronological work on the Boulder batholith and smaller associated stocks in southwestern Montana reveal a dominant age cluster around ~70–75 Ma (Lund et al., 2002, 2018; Schwartz, Schwartz et al., 2019), which suggests that local igneous doming is much younger than previously inferred by this depositional model. Alternative interpretations for thickness variations are that the strata were deposited atop a dissected pre-Cretaceous surface with notable relief and subtle local topographic highs (Dolson & Piombino, 1994) or an irregular flexural forebulge (Carrapa et al., 2019; DeCelles & Giles, 1996; Fuentes et al., 2011).

2.5. Depositional Age of the Kootenai Formation

The depositional age of the Kootenai Formation is assigned as Early Cretaceous (Aptian) based on stratigraphic position and early paleontological studies on the calcareous members (Cobban, 1955; Peck, 1941, 1951; Stanton, 1903; Yen, 1949, 1951). Sparse palynological constraints from the lower intervals of the formation, however, are considered slightly older than Aptian in age (Burden, 1984; DeCelles, 2004; Fuentes et al., 2009, 2011). Similarly, palynology of the chronostratigraphically equivalent Manville Group to the north in Alberta also suggests Early Cretaceous ages between Valanginian and early Albian (Burden, 1984; Mudge & Rice, 1982; Singh, 1964). Some workers have applied detrital zircon U-Pb analysis to sandstones in the Kootenai Formation, which has yielded a range of maximum depositional ages (MDAs) from ca. 140 to 107 Ma (Table 1; Fuentes et al., 2009; Laskowski et al., 2013; Quinn et al., 2018). More recently, a detailed measured section was analyzed from the Ziegler Gulch locality (Figures 2 and 4; Finzel & Rosenblume, 2021). This section was chosen because it occurs in some of the thickest and westernmost-preserved portions of the Kootenai Formation in southwestern Montana. As such, it likely contains one of the longest-duration records of distal foredeep sedimentation in the region. This measured section provides stratigraphic constraints and U-Pb detrital zircon (MDAs) for all four informal members of the formation; estimated ages are as follows: ~135 Ma for the Lower clastic member, ~115 Ma for the Lower calcareous member, ~112 Ma for the Upper clastic member, and ~110 Ma for the Upper calcareous member (gastropod limestone). These MDAs are consistent with ages determined by previous paleontological work; however, the age of the lowermost interval of the Kootenai Formation remains subject to considerable uncertainty because it generally lacks Cretaceous zircon grains.

3. Methods

3.1. Field Methods

Field localities were selected from a broad geographic area in southwestern Montana based on previous stratigraphic work and mapped outcrop belts of Lower Cretaceous strata (Figure 2; Table 1; DeCelles, 1984, 1986; Schwartz, 1972; Schwartz & DeCelles, 1988; Suttner, 1969). A stratigraphic section was measured and described at each locality to provide context for samples (Figure 4); each sample is identified by an abbreviation for the locality followed by the stratigraphic level from which it was collected in meters above the base. For one of the localities, a stratigraphic section was not measured, and the sample name does not include the meter number. Additional measured sections, locality data, and photographs are provided in the Supporting Information.

3.2. Sandstone Petrography

Standard thin sections of sandstones from the Kootenai Formation ($N = 22$) were prepared by Spectrum Petrographics. The Gazzi-Dickinson point counting method ($n = 400$) was followed to collect framework grain abundances from each of the thin sections (e.g., Ingersoll et al., 1984) using a Nikon Eclipse 50i POL polarizing microscope, PetrologLite x64 software, and an automated stepping stage. Framework grain abundances are presented on QFL and LmLvLs ternary diagrams following the scheme proposed by Garzanti (2019), which places chert in the lithic category. Sandstone thin sections accompany all detrital zircon samples,

Table 1
Compilation of U-Pb Detrital Zircon Data from the Kootenai Formation in Western Montana

Locality	Sampled interval	Sample ID	Type	YSG	YPP	Latitude	Longitude	Reference
Northwestern Montana								
Great Falls	Upper Kootenai sandstone; 5th member	ULK056 ($n = 283$)	III	101.2 ± 2.6	107 ($n = 36$)	47.53586	−111.20501	Quinn et al. (2018)
Great Falls	Red sandstone; 4th member	UK055 ($n = 249$)	III	105.4 ± 3.9	107 ($n = 43$)	47.56723	−111.10276	Quinn et al. (2018)
Gibson Reservoir	Middle Kootenai sandstone	1FG70 ($n = 99$)	III	104.3 ± 4.0	113 ($n = 33$)	47.61111	−112.74916	Fuentes et al. (2009)
Great Falls	Sunburst member sandstone	UK054 ($n = 244$)	I	136.7 ± 4.1	--	47.56698	−111.10306	Quinn et al. (2018)
Gibson Reservoir	Basal Kootenai sandstone	1SFSR1 ($n = 97$)	II	131.6 ± 4.5	134 ($n = 2$)	47.62972	−112.85888	Fuentes et al. (2011)
Gibson Reservoir	Basal Kootenai sandstone	1GR100 ($n = 95$)	II	141.1 ± 8.5	--	47.60250	−112.78083	Fuentes et al. (2009)
Great Falls	Cutbank member sandstone	GRF ($n = 91$)	I	139.3 ± 9.4	--	47.35188	−110.89320	Leier and Gehrels (2011)
Great Falls	Cutbank member sandstone	UK053 ($n = 256$)	I	--	--	47.25169	−111.42097	Quinn et al. (2018)
Great Falls	Cutbank member sandstone	UK052 ($n = 266$)	I	--	--	47.37952	−110.92316	Quinn et al. (2018)
Southwestern Montana								
Cinnabar Mountain	Upper clastic sandstone	CMK-1m ($n = 593$)	III	105.1 ± 1.2	110 ($n = 114$)	45.08895	−110.79099	This study
Ziegler Gulch	Gastropod limestone	ZG-271m ($n = 63$)	--	105.5 ± 4.7	110 ($n = 10$)	45.46912	−112.57951	Finzel and Rosenblume (2021)
Ziegler Gulch	Upper clastic sandstone	ZG-186m ($n = 546$)	II	105.7 ± 7.7	112 ($n = 30$)	45.46864	−112.57796	Finzel and Rosenblume (2021); This study
Ziegler Gulch	Lower micritic limestone	ZG-150m ($n = 32$)	--	105.8 ± 7.4	115 ($n = 12$)	45.46817	−112.57720	Finzel and Rosenblume (2021)
Tendoy Mountains	Middle Kootenai sandstone	10DM25 ($n = 86$)	I	119.2 ± 8.4	124 ($n = 10$)	44.71555	−112.80515	Laskowski et al. (2013)
Sappington	Lower clastic sandstone	SK-20m ($n = 563$)	II	120.6 ± 3.4	126 ($n = 9$)	45.81371	−111.80045	This study
Trapper Creek	Lower clastic sandstone	TCKKLC ($n = 284$)	II	129.1 ± 1.4	130 ($n = 6$)	45.63019	−112.72511	This study
Ziegler Gulch	Lower clastic sandstone	ZG-15m ($n = 565$)	II	129.3 ± 5.4	135 ($n = 5$)	45.46715	−112.57448	Finzel and Rosenblume (2021); This study
Frying Pan	Lower clastic sandstone	FPK-8m ($n = 575$)	II	140.0 ± 5.7	--	45.28588	−112.78177	This study
Lima Peaks	Lower clastic sandstone	LPK-1m ($n = 553$)	II	143.7 ± 1.6	144 ($n = 2$)	44.53062	−112.52951	This study
Nada Mine	Lower clastic sandstone	NM-18m ($n = 576$)	II	140.2 ± 7.0	145 ($n = 4$)	46.13026	−111.73626	This study
Cramp Spring	Lower clastic sandstone	CS-23m ($n = 558$)	II	--	--	46.01971	−111.46960	This study
Ruby River	Lower clastic sandstone	RRK-11m ($n = 524$)	I	--	--	45.05121	−112.00656	This study
Bridger Range	Pryor conglomerate	Kk ($n = 300$)	I	--	--	45.91026	−110.96175	Ronemus et al. (2020)

Table 1
Continued

Locality	Sampled interval	Sample ID	Type	YSG	YPP	Latitude	Longitude	Reference
Bridger Mountain	Pryor conglomerate	BRM (n = 98)	I	--	--	45.33272	−108.80448	Leier and Gehrels (2011)
Taylor Fork Creek	Basal Kootenai conglomerate	TFI (n = 91)	I	--	--	45.06136	−111.26474	Leier and Gehrels (2011)

Note. Samples are listed in stratigraphic order based on region. Refer to results section and Table 2 for description of types. Maximum depositional ages (MDAs) are estimated for samples containing Cretaceous grains; -- = indicates that an MDA was not estimated because that sample lacks Cretaceous grains. YSG = youngest single grain (Ma); YPP = youngest graphical peak (Ma); n = total number of individual grain analyses; sample coordinates are listed as decimal degrees in NAD83.

and for some measured sections, additional thin sections were collected from multiple stratigraphic levels (Figure 4). Framework grain abundance data are tabulated in the Supporting Information.

3.3. U-Pb Geochronology of Detrital Zircon Grains

Ten samples were collected for detrital zircon U-Pb geochronology. Most samples were collected from sandstones that directly overlie the basal conglomerate of the Lower clastic member (Figure 4). This member was sampled because it is the most consistent and recognizable clastic unit in the formation throughout the region. Therefore, we infer that it likely contains the most widespread record of initial foredeep sedimentation. At localities where the basal conglomerate was covered or otherwise unidentified, the lowermost prominent sandstone was sampled. At the Ziegler Gulch locality (Figure 2), a sample was also collected from the Upper clastic member. Detrital zircon grains were separated from ~5 to 7 kg of fist-sized pieces via the following mineral separation protocols. A jaw-crusher was used to reduce the sample to gravel-sized particles and a pulverizer was used to further reduce those particles to individual mineral grains. Grains were then separated into density fractions using a Gemini table; the densest fraction was sieved to <350 μm. The <350 μm fraction was passed through free fall and barrier Frantz magnetic separators to concentrate minerals with low magnetic susceptibility. Heavy liquid separation using methylene iodide (SG ~3.3) was performed for further concentration of the densest fraction. If present, opaque minerals were removed from the separate by hand and the remaining grains were poured and mounted with standards in a 1" epoxy mount following protocols used at the University of Arizona LaserChron Center. Ring mounts were polished to expose grain cores and backscattered electron images were acquired using a Hitachi S-3400N scanning electron microscope at the University of Iowa.

Detrital zircon grains were analyzed following standard protocols at the University of Arizona LaserChron Center using both a Nu HR laser ablation-multicollector-ICPMS and a Thermo Element2 single-collector ICPMS (Gehrels et al., 2008; Gehrels & Pecha, 2014; Pullen et al., 2018; Sundell et al., 2020). The Nu HR was used to acquire the nine large-n data sets (n = 600), whereas the Element2 was used to collect one moderate-n data set (n = 300). Reference materials used for Nu HR analyses were Duluth Gabbro (FC) zircon (~1,099 Ma) and R33 (~420 Ma), whereas Element2 analyses included a third reference material, Sri Lanka (SL) zircon (~563.5 Ma). U-Pb data collected using the Nu HR were reduced and filtered using the AgeCalcML Nu Time Resolved Analysis MATLAB script (Sundell et al., 2020). Data collected using the Element2 were reduced and filtered using Arizona's internal E2AgeCalcExcel spreadsheet. The following filters were applied to all data collected for this study. Analyses with elevated levels of ^{204}Pb were filtered from the data set using a 600-cps ^{204}Pb filter for the Nu HR data and a ^{206}Pb/^{204}Pb filter of 200 for the Element2 data. A correction for ^{204}Pb was applied to the remaining data using a ^{206}Pb/^{204}Pb factor of 1 (Stacey & Kramers, 1975). An uncertainty cutoff of 10% was applied to ^{206}Pb/^{238}U and ^{206}Pb/^{207}Pb ratios collected from standards. Unknowns with greater than 10% discordance or 5% reverse discordance for ages older than 600 Ma were filtered from the data set; discordance was not calculated for grains younger than 600 Ma because measurement of ^{207}Pb from small volumes of ablated material using LA-ICPMS is challenging (e.g., Spencer et al., 2016). Best ages are presented as ^{206}Pb/^{238}U ages for grains younger than 900 Ma and ^{207}Pb/^{206}Pb ages for grains older than 900 Ma because that cutoff does not artificially divide an age cluster (Gehrels et al., 2008).

3.4. Statistical Analyses of U-Pb Age Spectra

Multi-dimensional scaling (Vermeesch, 2013) was used to aid visual comparison among the Kootenai Formation detrital zircon age data. This technique allows for detrital zircon age distributions to be grouped statistically based on their relative dissimilarities through calculation of a cross-correlation matrix, which is best visualized in two- or three-dimensional Euclidean space (e.g., Saylor & Sundell, 2016). The result is a dimensionless plot on which samples that are similar fall near each other, whereas those that are dissimilar plot far from each other. In this study, we employ a MATLAB-based multi-dimensional scaling tool (Saylor et al., 2017) to compare our new detrital zircon age spectra with additional data sets from the literature based on cross-correlation of probability density plots using the metric squared stress criterion.

Provenance mixture modeling was applied to the age spectra with the aim of quantifying relative contributions from specific sediment sources to the basinal strata. In theory, as source areas are eroded and detritus is transported to the sink, the complete detrital zircon signature of each source should be recycled into the basin (e.g., Hadlari et al., 2015; Schwartz, Schwartz et al., 2019). We employed an inverse Monte Carlo mixture model (Sundell & Saylor, 2017), which varies the relative contributions of each detrital zircon spectrum from a group of potential sedimentary source spectra to create a best fit model for a mixed detrital zircon sample. Ten thousand iterations were performed for each model, each one consisting of different relative proportions of source area mixtures, and the best 1% of those iterations were identified through comparison with basin strata signatures. The best fit model was evaluated using a cross-correlation coefficient (R^2) that compares the probability values of the basin sample with those of the best fit model. Based on the n-value ($n = 600$) of the detrital zircon U-Pb age spectra that were run through the mixture modeling software, we consider $R^2 > \sim 0.70$ to indicate that most of the potential sediment sources have been identified and are reasonably represented in the model, whereas $R^2 < \sim 0.70$ may indicate that some of the potential sources have not been identified or are under-represented in the source strata data set (e.g., Saylor & Sundell, 2016).

4. Results

4.1. Sandstone Petrography

We present modal petrographic data from 22 thin sections of sandstones collected mainly from the Lower clastic member of the Lower Cretaceous Kootenai Formation in southwestern Montana (Figure 4; Supporting Information). In the westernmost reaches of the study area, where a distinct Upper clastic member is present, additional samples were collected to check for upsection variability. Our analysis reveals three types of sandstone within the Kootenai Formation that occur throughout southwestern Montana (Figure 5): quartz-rich (Type I), sedimentary lithic-rich (Type II), and those that contain feldspars and minor volcanic lithics (Type III). Based on previous interpretations, all sampled sandstones for this study were deposited in nonmarine settings (DeCelles, 1986). Framework grain abundance (Figure 6) for each type is presented as QFL and LmLvLs percentages (after Garzanti, 2019); detailed grain count data are available in the Supporting Information. New sandstone types were compared with existing published data from the same stratigraphic levels and based on this comparison, Types I and II are present throughout much of western Montana, whereas Type III more commonly occurs in northwestern Montana (Fuentes et al., 2011; Quinn et al., 2018).

4.1.1. Type I Sandstone

Type I sandstone ($N = 2$) occurs locally at the base of the Kootenai Formation and is generally more compositionally mature than Types II and III. It is typically well-sorted and quartz-rich, with sub-rounded to well-rounded grains; previous workers have interpreted deposition in a nonmarine setting (DeCelles, 1986). Comparison of our Type I samples with previously published petrographic data from Kootenai Formation and equivalent sandstones indicates that this type occurs from western Montana to northern British Columbia, where sandstones were deposited in marginal to shallow marine settings (Gillespie, 1992; Leier & Gehrels, 2011; Quinn et al., 2016, 2018; Raines et al., 2013; Schwartz & Vuke, 2019; Walker, 1974). Quartz-rich sandstones are also common near Great Falls, Montana, where they are reflective of nonmarine and marginal marine settings (e.g., Quinn et al., 2018); however, this type of sandstone was not documented near Gibson Reservoir (Figure 2) and may be more prevalent in the east (Fuentes et al., 2011). In our samples, Type I sandstone was only identified at the Ruby River locality (Figure 2; RRK). Framework grain

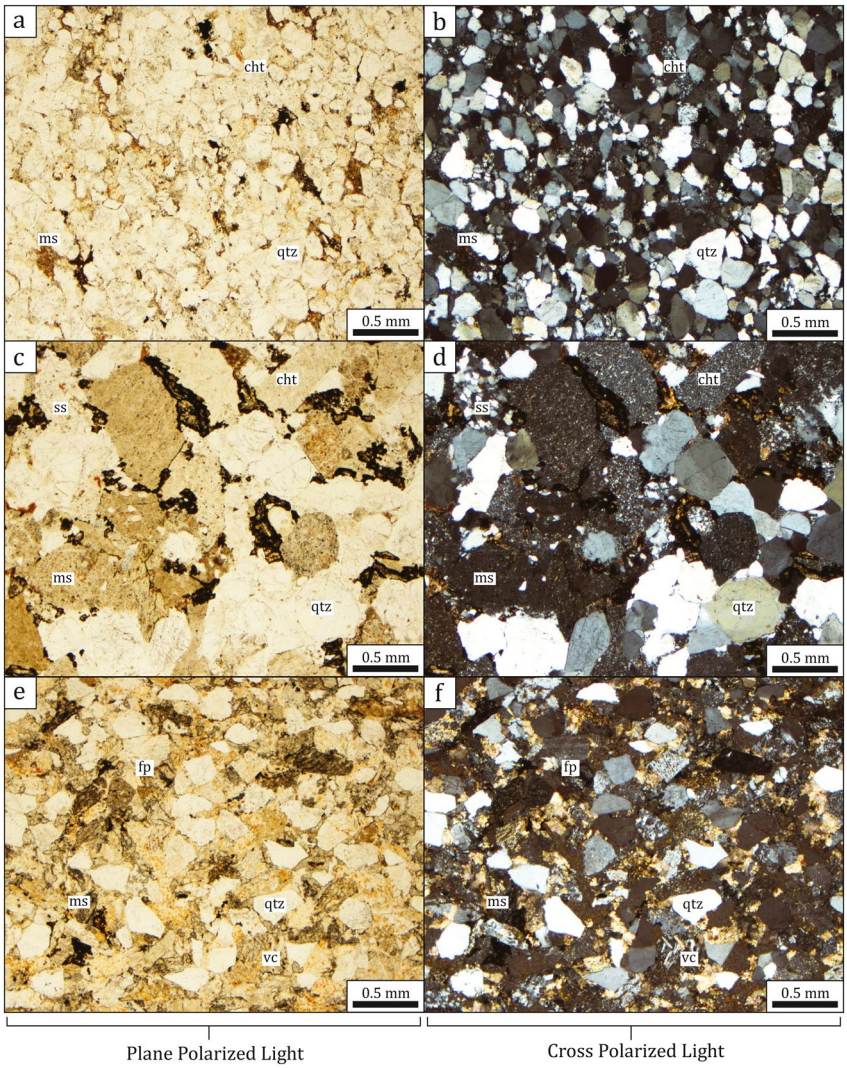

Figure 5. Representative thin section photomicrographs of Kootenai Formation sandstones. (a), (b) Type I: fine-grained quartz-rich sandstone from RRK-11m locality. (c), (d) Type II: coarse-grained lithic-rich sandstone from ZG-15m locality. (e), (f) Type III: sandstone containing feldspars and volcanic lithics from CMK-1m locality. Abbreviations are as follows: cht (chert), fp (plagioclase feldspar), ms (mudstone), ss (sandstone), qtz (quartz), vc (volcanic).

abundances in our two samples range from 77% to 89% quartz and 11%–23% lithics; the average composition is 83% quartz and 17% lithics. Lithics from these sandstones are 100% sedimentary; they mainly consist of chert and mudstone. In comparison, only five of the 68 thin sections presented by Schwartz and DeCelles (1988) contain >80% quartz; they range from 83% to 92% quartz and 8%–17% lithics; the average composition is 89% quartz and 11% lithics (refer to the Supporting Information for these data).

4.1.2. Type II Sandstone

Type II sandstone ($N = 19$) has a salt-and-pepper appearance in hand sample due to abundant lithic grains and generally represents the bulk of our Kootenai Formation samples in southwestern Montana. These sandstones range from fine-to coarse-grained and are petrographically distinct from the other types because they contain notable abundances of chert and mudstone lithics; previous workers interpreted that they were deposited in nonmarine settings (e.g., DeCelles, 1986). Sedimentary lithic-rich or chert-rich sandstones that we characterize here as Type II sandstones have been recognized in Lower Cretaceous strata by many other workers in northwestern (e.g., Ballard, 1966; Fuentes et al., 2011; Gillespie, 1992; Harris, 1968) and southwestern Montana (e.g., DeCelles, 1986; Schwartz, 1983; Suttner, 1969; Suttner et al., 1981).

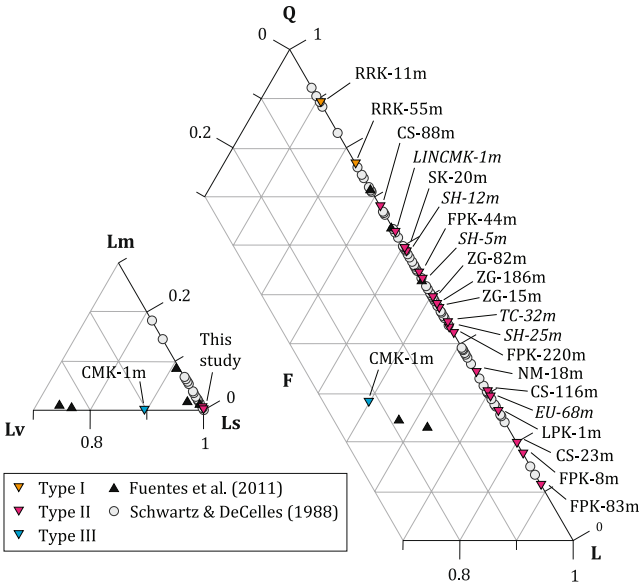

Figure 6. Ternary diagrams displaying recalculated Kootenai Formation grain count data from this study incorporated with additional data from the literature. Italicized samples are from measured sections that are not shown in Figure 4. Note that 21 of 22 thin sections analyzed in this study contained >99% sedimentary lithics. Abbreviations are as follows: Q (quartz), F (feldspar), L (lithics), Lm (metamorphic lithics), Lv (volcanic lithics), Ls (sedimentary lithics).

Additionally, chert-rich sandstones are present in Lower Cretaceous rocks from south-central Alberta to northern British Columbia (Hopkins, 1981; Raines et al., 2013). In our study, Type II framework grain abundances range from 11% to 68% quartz and 32%–89% sedimentary lithics; average composition is 42% quartz and 58% sedimentary lithics. Lithics in these sandstones are 100% sedimentary; they mainly consist of chert, mudstone, and minor sandstone. When compared with Kootenai Formation petrographic data from the literature (Figure 6), there is notable overlap. Three thin sections from Fuentes et al. (2011), which we classify as Type II, range from 53% to 72% quartz, <1% feldspar, and 28%–46% lithics; the average composition is 63% quartz and 37% lithics. Sixty three of the 68 total thin sections presented by Schwartz and DeCelles (1988) contain <80% quartz; they range from 14% to 76% quartz and 24%–86% lithics and the average composition is 48% quartz and 52% lithics (refer to Supporting Information for classification table).

4.1.3. Type III Sandstone

Type III sandstone ($N = 1$) was collected near Cinnabar Mountain (Figure 2), where a red sandstone is overlain by a thin limestone (Figure 4); the unit is mapped as Kootenai Formation (Berg et al., 1999) and represents the stratigraphically highest of the three sandstone types. The sandstone contains angular grains that are fine-to-medium in size in addition to feldspar and minor volcanic lithics; it was also deposited in a nonmarine setting (Schwartz, 1972). Though some workers (Fox & Groff, 1966; Fuentes et al., 2011; Gillespie; 1992; Hayes, 1986) documented the presence of feldspar and volcanic lithics in upper Kootenai Formation sandstones from northwestern Montana, prior to our study, this type of sandstone had not been documented in Kootenai Formation strata in southwestern Montana. In our samples, Type III sandstone was only identified at the Cinnabar Mountain locality (Figure 2; CMK). Framework grain abundances are 28% quartz, 22% feldspar, and 50% lithics, which is consistent with observations from the literature. Lithics in these sandstones are 90% sedimentary and 10% volcanic; sedimentary lithics consist mainly of mudstone and chert. The average of two thin sections from Fuentes et al. (2011), which we classify as Type III (refer to the Supporting Information), is 24% quartz, 6% feldspar and 60% lithics, which were designated as <1% metamorphic, 24% volcanic, and 75% sedimentary. The two thin sections described by Fuentes et al. (2011) plot near our CMK-1m sample on the ternary diagram (Figure 6).

4.2. U-Pb Ages From Detrital Zircon Grains

We present U-Pb detrital zircon data from 10 new samples ($n = 5{,}337$ individual analyses) collected from the Lower Cretaceous Kootenai Formation in southwestern Montana (Figure 7; Table 1). We integrate these new data with existing U-Pb detrital zircon data compiled from the literature. A combination of multi-dimensional scaling, visual analysis of the detrital zircon age data, and identification of statistically significant populations using AgePick (Gehrels, 2010) reveals three distinctly different age spectra (Figure 8). Here, we present the detrital zircon data as integrated regional composites. The three different spectra types represent a general upsection progression through the formation, but they are also spatially controlled. Type I mostly occurs in the east and only locally in the west, Type II is mainly restricted to the west, and Type III is largely present in the north, however, it also occurs in the southeasternmost sample in our study area (Figure 2). Importantly, each detrital zircon type signature directly corresponds to the same petrographically determined sandstone type (Table 2). For the purposes of comparison among the regional composites, we employ three broad age groups: Archean-Paleoproterozoic (>1,600 Ma), Mesoproterozoic-early Paleozoic (1,600–330 Ma), and Permian-Cretaceous (299–100 Ma). For our detailed analysis, however, 10 age groups are shown in each pie diagram (Figure 7).

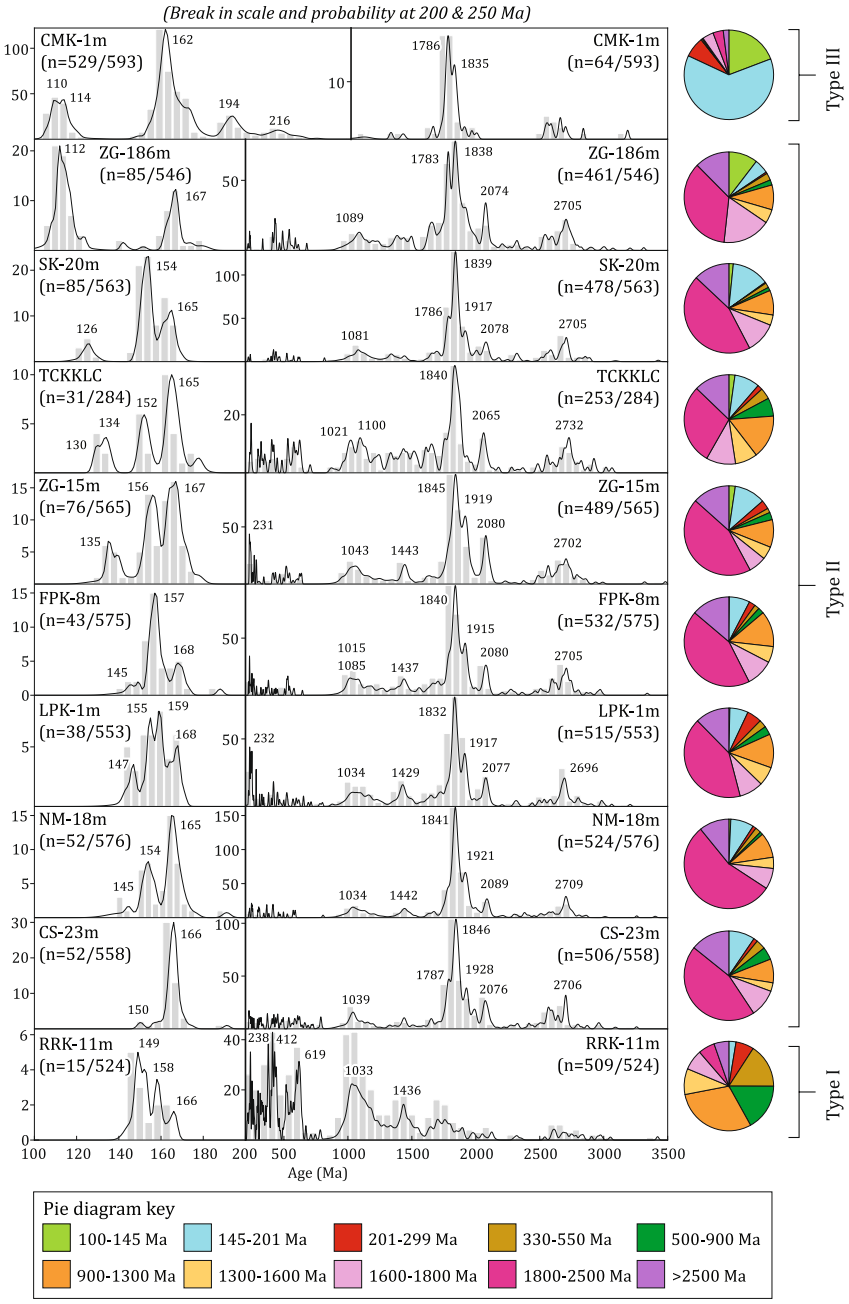

Figure 7. Detrital zircon probability density plots and pie diagrams displaying new data collected from the Kootenai Formation for this study. The central black vertical line indicates a break in scale and probability. Along the *x*-axis, a break was placed at 200 Ma for most samples; however, for CMK-1m, a break was placed at 250 Ma to avoid artificially dividing an age group. There are two separate *y*-axes; the far left *y*-axis denotes the number of grains in the histograms of the younger age fractions, wheres the *y*-axis along the central vertical line denotes the number of grains in the histograms of the older age fractions. The number of grains (*n*-value) in each age fraction is listed separately.

4.2.1. Type I Regional Composite

Nine detrital zircon samples constitute the Type I regional composite signature ($n = 1{,}956$): one sample from this study and eight samples from the literature (Figure 8b; Table 2). Samples designated as Type I are present throughout the region and mainly occur within the Basal/Pryor conglomerate, Lower clastic, Cutbank, and Sunburst-Great Falls members (Figure 3). This signature is typified by a dominant population of Mesoproterozoic-early Paleozoic ages that constitute 60% of the composite signature; Archean-Paleoproterozoic

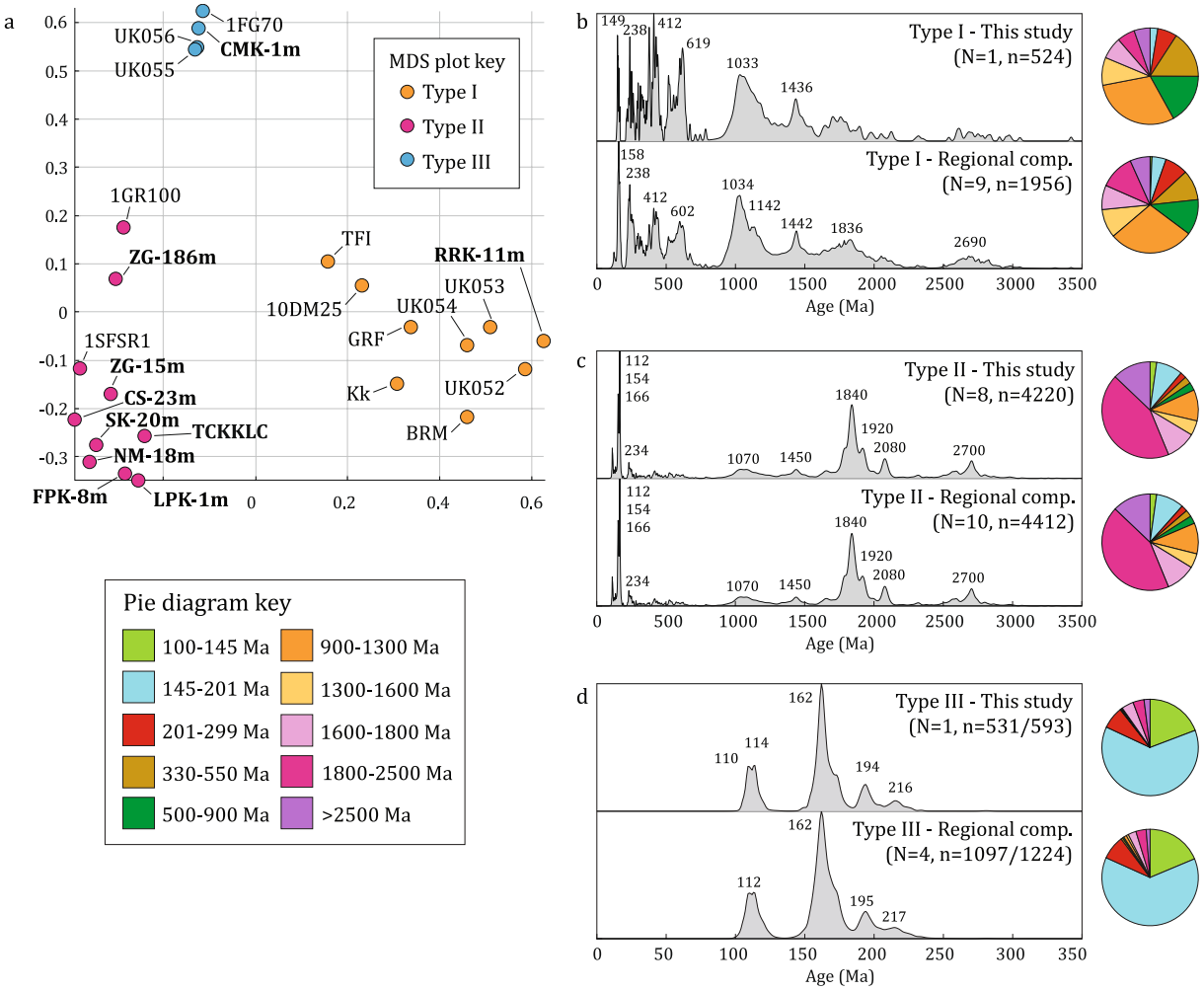

Figure 8. Type signatures of Kootenai Formation sandstones based on detrital zircon analysis. Data from this study are compared with regional composite signatures, which are compilations of all samples shown on the MDS plot. (a) Results of metric squared stress multi-dimensional scaling analysis; samples from this study are bolded. (b) Type I detrital zircon probability density plots and pie diagrams. (c) Type II detrital zircon probability density plots and pie diagrams. (d) Type III detrital zircon probability density plots (<350 Ma) and pie diagrams (0–3,500 Ma); the *x*-axis for the Type III is different to show an expanded view of the most abundant ages in the composite (refer to Figure 9 for the older age fraction of the Type III regional composite).

ages (27%) and Permian-Cretaceous ages (13%) make up lesser proportions. In our samples, dated detrital zircon grains are generally rounded and elongate and exhibit mostly clear to light gray and rare pink colors. The key characteristics for the Type I signature are dominant age peaks at ca. 158, 238, 412, 602, and 1,034 Ma, as well as minor peaks at 1,142, 1,442, 1,836 and 2,690 Ma. Type I sandstones are generally fine-grained and framework grains are dominated by monocrystalline quartz.

4.2.2. Type II Regional Composite

Ten detrital zircon samples constitute the Type II regional composite signature (n = 4,220): eight samples from this study and two samples from the literature (Figure 8c; Table 2). Samples designated as Type II compose the bulk of the Kootenai Formation in southwestern Montana, nine of them are from sandstone in the Lower clastic member and one (ZG-186m) is from sandstone in the Upper clastic member (Figure 3); all are lithic-rich. In contrast to the Type I signature, the Type II signature is characterized by a dominant population of Archean-Paleoproterozoic ages that constitute 66% of the composite signature; Mesoproterozoic-early Paleozoic ages (20%) and Permian-Cretaceous ages (14%) make up lesser proportions. Dated detrital zircon grains from this study are generally rounded and elongate with rare euhedral shapes and are clear to light gray, pink and purple in color. The key characteristics for the Type II signature are dominant age peaks

Table 2
Regional Composite Type Signatures Based on Combined Sandstone Petrography and U-Pb Detrital Zircon Ages

Regional composite	Inclusive detrital zircon samples	Major age groups in regional composite (%)	QFL (average %)	Key features in regional composites
Type I	10DM25[c], BRM[d], GRF[d], Kk[f], **RRK-11m**, TFI[d], UK052[e], UK053[e], UK054[e] (this study: $N = 1$, $n = 524$; regional composite: $N = 9$, $n = 1{,}956$)	Permian-Cretaceous – 13% Mesoproterozoic-early Paleozoic – 60% Archean-Paleoproterozoic – 27%	Q – 87% F – 0% L – 13%	Mesoproterozoic-early Paleozoic ages with significant ca. 1040 Ma peak; fine-grained quartz-rich sandstone
Type II	1GR100[a], 1SFRSR1[b], **CS-23m, FPK-8m, LPK-1m, NM-18m, SK-20m, TCKKLC, ZG-15m, ZG-186m** (this study: $N = 8$, $n = 4{,}220$; regional composite: $N = 10$, $n = 4{,}412$)	Permian-Cretaceous – 14% Mesoproterozoic-early Paleozoic – 20% Archean-Paleoproterozoic – 66%	Q – 47% F – 0% L – 53%	Archean-Paleoproterozoic ages with significant ca. 1850 Ma peak; abundant sedimentary lithics in sandstone
Type III	1FG70[a], **CMK-1m**, UK055[e], UK056[e] (this study: $N = 1$, $n = 593$; regional composite: $N = 4$, $n = 1{,}224$)	Permian-Cretaceous – 90% Mesoproterozoic-early Paleozoic – 3% Archean-Paleoproterozoic – 7%	Q – 25% F – 18% L – 57%	Dominance of Mesozoic ages with significant ca. 160 Ma peak; feldspars and minor volcanic lithics in sandstone

Note. New samples from this study are bolded.
[a]Fuentes et al. (2009). [b]Fuentes et al. (2011). [c]Laskowski et al. (2013). [d]Leier and Gehrels (2011). [e]Quinn et al. (2018). [f]Ronemus et al. (2020).

at ca. 154, 166, 1,840, 1,920, 2,080, and 2,700 Ma, minor peaks at 1,070 and 1,450 Ma, and an abundance of sedimentary lithic framework grains.

4.2.3. Type III Regional Composite

Four detrital zircon samples constitute the Type III regional composite signature ($n = 1{,}224$): one sample from this study and three samples from the literature (Figure 8d; Table 2). Samples designated as Type III are present throughout western Montana and are all from sandstone in the upper part of the Kootenai Formation. In contrast to the Type I and II signatures, Type III is characterized by a dominant population of Permian-Cretaceous ages that constitute 90% of the composite signature; Archean-Paleoproterozoic ages (7%) and Mesoproterozoic-early Paleozoic ages (3%) make up minor proportions. A distinction of this signature is that the pre-Mesozoic age groups form a strong peak around 1,780 Ma (Figure 9), whereas that age is less prominent in Types I and II. Dated detrital zircon grains from this study are dominantly euhedral to subhedral with a minor rounded population and are mainly clear to light gray and rarely pink in color. The key characteristics for the Type III signature are dominant age peaks at ca. 112 and 162 Ma, minor peaks at 195, 217 and 1,780 Ma, and framework grains including feldspar and minor volcanic lithics.

5. Interpretations

5.1. Maximum Depositional Ages

The youngest single grain (YSG) and youngest graphical peak (YPP) were compiled for all samples used in this study with an aim to provide conservative MDA estimates for the entire data set (Table 1; Dickinson & Gehrels, 2009b). The detailed section at the Ziegler Gulch locality (Figures 2 and 4) provides a chronostratigraphic framework within which we place the interpreted ages of our samples (Finzel & Rosenblume, 2021). Six of the 10 samples from this study provide new depositional age information (Table 1). YPPs were estimated for four of those samples; however, two yielded only a single Cretaceous grain. For these samples, we interpret that the YSG approach may be unreliable due to Pb-loss and reproducibility (e.g., Coutts et al., 2019; Spencer et al., 2016). Overall, near depositional-age grains are scarce to limited in the lower intervals of the formation but become increasingly abundant upsection. Our new MDAs from southwestern Montana progressively young upsection from ~145 to 110 Ma and are consistent with the chronostratigraphic framework established by the Ziegler Gulch measured section and existing age constraints.

10.1029/2020TC006561

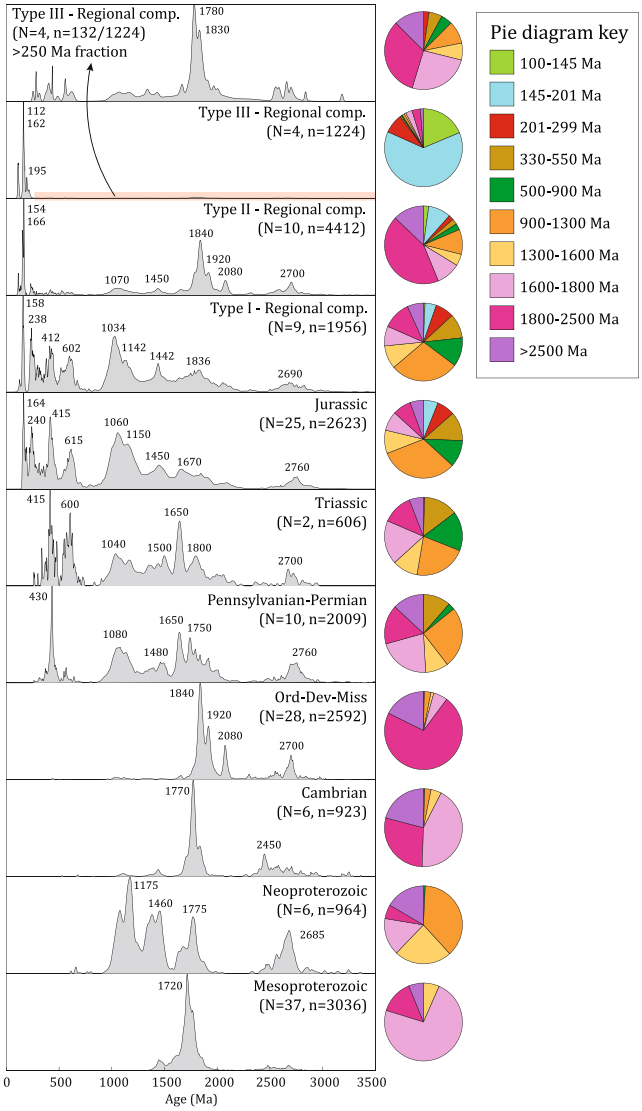

Figure 9. Type composites from this study compared with potential sources for recycled detrital zircon grains from the Idaho-Montana sector of the Sevier fold-thrust belt and Colorado Plateau highland region. Data are displayed as composite detrital zircon probability density spectra and pie diagrams. These potential source composites were used as inputs for the mixture models; they are shown as multicolored spectra in Figure 10. References are as described in Section 5.2.

5.2. Potential Sediment Sources

Potential sources of recycled detrital zircon for the Kootenai Formation are Mesoproterozoic rift-related and Neoproterozoic-Paleozoic passive margin strata within the Idaho-Montana sector of the Sevier fold-thrust belt and Jurassic strata of the Colorado Plateau, all of which were exhumed by Cordilleran mountain building during Early Cretaceous time (Dickinson & Gehrels, 2008; Fuentes et al., 2011). Detrital zircon U-Pb data from these potential source strata were compiled from previous studies and new samples were collected from the Pennsylvanian Quadrant, Permian Phosphoria, and Triassic Dinwoody formations in southwestern Montana where existing published data are limited (Supporting Information). Previous workers have interpreted a variety of sources for the Kootenai Formation including recycled Mesoproterozoic-Mesozoic strata (DeCelles, 1986; Fuentes et al., 2011; Laskowski et al., 2013; Quinn et al., 2018; Schwartz & DeCelles, 1988; Suttner, 1969). Based on the variability of those previous interpretations, we compiled seven main source composites with the aim of testing all the potential sources in the Idaho-Montana region. These source strata composites were grouped based on characteristic age peaks that occur in their detrital zircon age spectra (Figure 9; Supporting Information). The Mesoproterozoic Belt-Purcell Supergroup composite ($N = 37$, $n = 3{,}036$) has a recognizable age peak at 1,720 Ma (Lewis et al., 2010; Link et al., 2007, 2016; Stewart et al., 2010). The Neoproterozoic strata composite ($N = 6$, $n = 964$) is multi-modal and has four main age peaks at 1,175, 1,460, 1,775, and 2,685 Ma; a local ~667 Ma tuff within the Neoproterozoic strata was not included in our source composite (Brennan et al., 2020). The Cambrian strata composite ($N = 6$, $n = 923$) is identifiable by a strong unimodal peak at 1,770 Ma (Brennan et al., 2020); data from Upper Cambrian strata (Link et al., 2017) were not included because they exhibit a prominent ~500 Ma peak that is not present in the Kootenai Formation and are otherwise indistinguishable from Lower Cambrian data. The Ordovician-Devonian-Mississippian strata composite ($N = 28$, $n = 2{,}592$) has distinctive age peaks of 1,840, 1,920, 2,080, and 2,700 Ma (Baar, 2009; Beranek et al., 2016; Brennan et al., 2020; Ma et al., 2016). The Pennsylvanian-Permian strata composite ($N = 10$, $n = 2{,}009$) is multi-modal with age peaks at 430, 1,080, 1,480, 1,650, 1,750, and 2,760 Ma (Leary et al., 2020; Link et al., 2014; this study). The Triassic strata composite ($N = 2$, $n = 606$) displays ages of 415, 600, 1,040, 1,500, 1,650, 1,800, and 2,700 Ma (this study). The Jurassic strata composite ($N = 25$, $n = 2{,}623$) age peaks are 164, 240, 415, 615, 1,060, 1,150, 1,450, and 1,670 Ma (Dickinson & Gehrels, 2008, 2009a; Fuentes et al., 2011; Quinn et al., 2018).

Potential first-cycle sources of the 160 and 115–110 Ma detrital zircon grains in the Kootenai Formation remain elusive. Some workers have interpreted that a predecessor phase to the Idaho batholith containing those ages may have been tectonically removed from the region or shortened and stretched along strike during Late Cretaceous time (Gaschnig et al., 2017; Giorgis et al., 2005, 2008). In contrast, other plutonic complexes in western North America such as the Sierra Nevada and Coast Mountains batholiths, have longer magmatic histories. For example, the Sierra Nevada batholith was active for >140 m.y., but most volcanic activity and/or shallow crustal magmatism was in the Late Jurassic (160–150 Ma) and the Late Cretaceous (100–85 Ma; Ducea, 2001). The Coast Mountains batholith records active magmatism from 177 to 162, 157–142, and 118–100, and 100–50 Ma (Gehrels et al., 2009).

Much of the modern-day extent of the Idaho batholith is younger than 100 Ma, with relatively few 160 and 110–120 Ma plutons, which have only been documented in the Hazard Creek complex of the Salmon River suture zone and in the structurally juxtaposed Wallowa terrane of the Blue Mountains province (Giorgis et al., 2008; McClelland & Oldow, 2007; Unruh et al., 2008). Except for these suture zone plutons, most ages from the modern-day outcrop exposure of the Idaho batholith are <100 Ma (Gaschnig et al., 2010), and therefore younger than the Kootenai Formation. Given that the suture zone plutons represent only the westernmost edge of the present-day extent of the Idaho batholith (Gaschnig et al., 2010), the majority of the batholith is excluded as a potential source. The Blue Mountains province is currently situated to the west of the study area; it is an early Mesozoic collisional island arc and forearc assemblage with a complex accretionary and translational history (e.g., Dorsey & LaMaskin, 2007; Gaschnig et al., 2017; Gray et al., 2019; LaMaskin et al., 2011; Schwartz et al., 2010). Mesozoic plutons of the Blue Mountains province represent a potential sediment source for the 160 Ma detrital zircon grains in the study area. However, the presence of dextral shear zones in western Idaho suggests that southern portions of the Omineca belt (Figure 1) may also represent a potential source for the Kootenai Formation (e.g., McClelland et al., 2000). The southern Omineca belt is a collision-related magmatic-metamorphic complex formed during Jurassic accretion of the composite Intermontane superterrane (Coney & Evenchick, 1994). Potential plutonic sources in this belt include the Nelson batholith and nearby plutons of southern British Columbia (Figure 1; Archibald et al., 1983; Carr, 1991; Ghosh, 1995; Hurlow, 1993; Sevigny & Parrish, 1993; Surpless et al., 2014; Webster et al., 2017). These potential source regions imply a northward continuation of dextral faults outboard of the Idaho batholith into southern British Columbia; these may include the Pasayten fault, which is a potential northward continuation of the western Idaho shear zone (Figure 1), and/or other undetected faults to the east within the extensional complexes of the southern Omineca belt (McClelland & Oldow, 2007).

5.3. Type I Provenance—Jurassic Continental Strata

In western Montana, most workers have interpreted the basal conglomerate of the Kootenai Formation to be sourced from recycled Jurassic aeolianite strata from the southwestern US based on detrital zircon U-Pb analysis (e.g., Dickinson & Gehrels, 2009a; Laskowski et al., 2013; Leier & Gehrels, 2011; Quinn et al., 2018; Ronemus et al., 2020). In our new and compiled data set, this detrital zircon signature mainly occurs near the base of the Kootenai Formation and only locally upsection throughout southwestern Montana; it is less common in the west than the east.

Consistent with the findings of previous workers, our mixture modeling of the composite Type I signature (Figure 10a) reveals that Jurassic strata are the dominant contributor, with only minor input from Pennsylvanian-Permian and Triassic strata. The Type I model results in a best fit with $R^2 = 0.801$ and indicates no to very little contribution from Mesoproterozoic, Neoproterozoic, Cambrian, or Ordovician-Devonian-Mississippian strata, and 4% from Pennsylvanian-Permian, 4% from Triassic, and 84% from Jurassic strata. Mixture modeling results are consistent with visual comparison of detrital zircon spectra (Figure 9), which reveals striking similarity between the Type I regional signature and Jurassic composite spectrum.

Petrographic analysis also supports a recycled Jurassic strata source. Jurassic aeolianites from the Colorado Plateau region are generally fine-to medium-grained, well-sorted, sub-rounded to rounded, and composed of ~85% quartz, ~10% feldspar and ~5% lithics (Dickinson & Gehrels, 2009a). In western Montana, the Jurassic Morrison Formation is quartz-rich, contains <5% feldspar and ~1%–10% lithics; however, it may locally contain up to ~40% lithics (Suttner, 1969). Fuentes et al. (2011) documented 85% quartz, 1% feldspar, and 14% total lithics from Jurassic sandstones in northwestern Montana. We find that our two Type I sandstone thin sections are consistent with these descriptions. The samples from the Ruby River locality (Figures 2 and 4; RRK-11m and RRK-55m) are fine-to very-fine grained, well-sorted, quartz-rich sandstones with only minor lithic fragments (Figures 5a and 5b).

5.4. Type II Provenance—Lower-Middle Paleozoic Strata in Idaho

The main clastic source for the Kootenai Formation has long been interpreted as eroded Pennsylvanian-Permian passive margin strata based on the presence of chert and quartzite clasts in the basal conglomerate and abundant chert lithic fragments in sandstone (Suttner, 1969). Metamorphic lithics in sandstone and

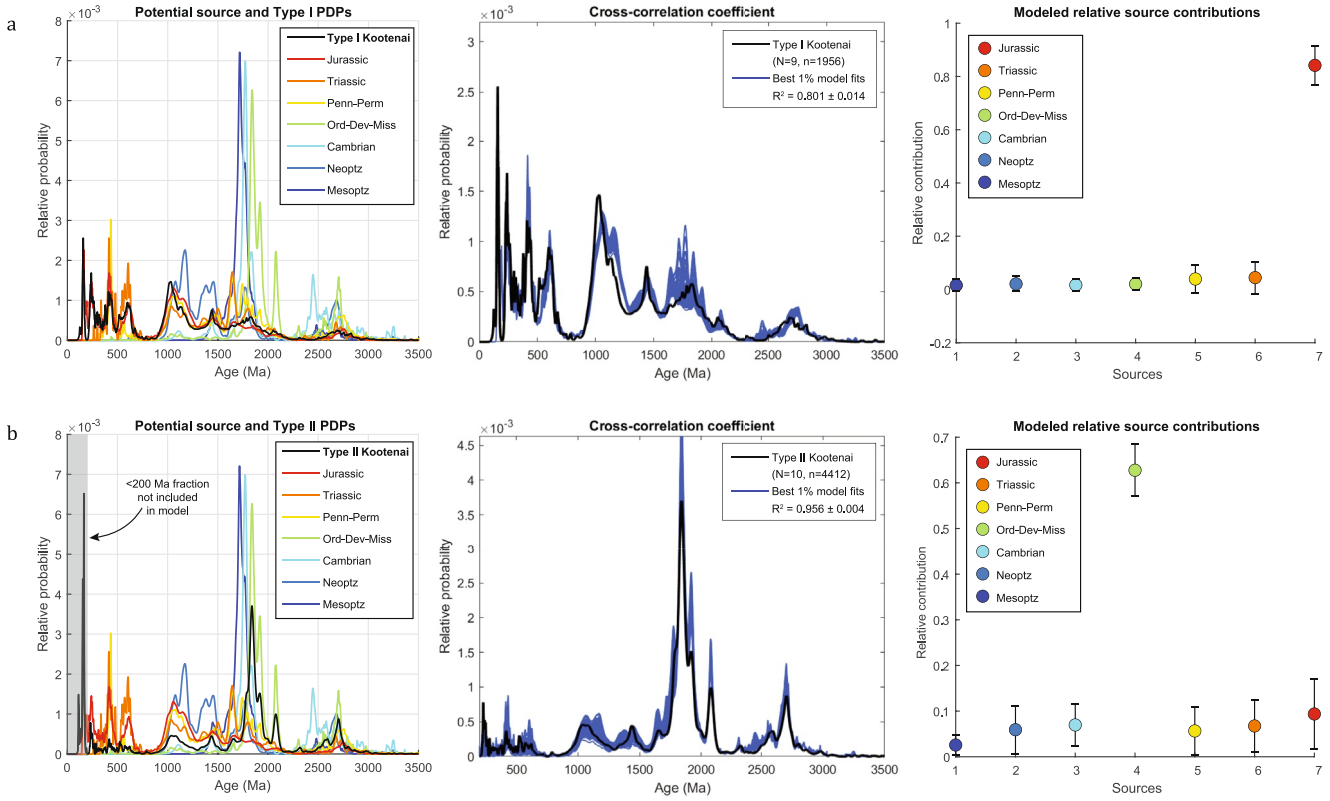

Figure 10. (a) Mixture model results for Type I regional composite signature. Refer to Figure 9 for characteristic ages of each U-Pb potential source spectrum. (b) Mixture model results for Type II regional composite signature; this model does not include the <200 Ma age fraction. Both rows contain three components: model input, output in graphical format, and output presented as modeled relative contributions from source strata.

1.7–1.9 Ga ages from detrital zircon grains have also been used to suggest the Mesoproterozoic Belt-Purcell Supergroup as a source for the fine-grained lithologies (DeCelles, 1986; Fuentes et al., 2011; Schwartz & DeCelles, 1988). However, structural analysis from northwestern Montana suggests exposure of dominantly Paleozoic miogeoclinal strata during Early Cretaceous time (Fuentes et al., 2012). Our findings contrast with previous provenance interpretations and instead indicate that a combination of recycled lower-middle Paleozoic strata that occur in east-central Idaho and Jurassic continental strata are a better fit for Type II sandstones.

We present a mixture model for the regional composite Type II U-Pb detrital zircon signature (Figure 10b) that suggests very little input from Mesoproterozoic-Cambrian strata. The <200 Ma age fraction was not included in our mixture model. The Type II mixture model results in a best fit with $R^2 = 0.956$ and indicates major contributions of 62% Ordovician-Devonian-Mississippian and 10% Jurassic strata. These results are consistent with visual comparison of detrital zircon spectra (Figure 9), from which distinctive age peaks of 1,840, 1,920, 2,080, and 2,700 Ma can be clearly recognized. These same age peaks are present in detrital zircon data from Ordovician, Devonian, and Mississippian strata located in east-central Idaho (Baar, 2009; Beranek et al., 2016; Brennan et al., 2020; Ma et al., 2016). Specifically, the Ordovician Kinnikinic Formation, Devonian Milligen Formation, and Mississippian Copper Basin Group have strikingly similar abundant Archean-Paleoproterozoic ages compared to the Type II samples. The Jurassic component in the Type II detrital zircon spectra is overwhelmed by older ages from the lower-middle Paleozoic strata and Cordilleran arc-derived ages of 154 and 166 Ma. However, the mixture models identify a Jurassic source based on three minor peaks between ca. 200–650 Ma and two recognizable peaks of ca. 1,070 and 1,450 Ma.

These interpretations are supported by sandstone petrography, which reveals grains that we attribute to lower-middle Paleozoic strata. The Ordovician Kinnikinic Formation is a white ridge-forming unit in east-central Idaho; in thin section it is described as fine-to medium-grained, locally coarse-to very coarse-grained,

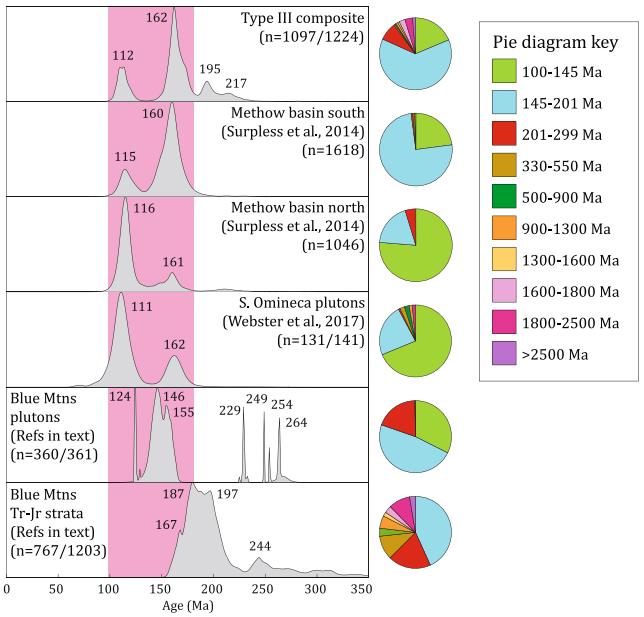

Figure 11. Type III regional composite detrital zircon probability density plot displaying most prominent age fractions (<350 Ma) and pie diagrams (0–3,500 Ma) compared with data from Cretaceous strata of the Methow basin, plutonic ages from the southern Omineca belt, plutonic ages in the Blue Mountains province, and potentially recycled Triassic-Jurassic strata of the Blue Mountains province. Purple shaded bar highlights the 110–115 and 160 Ma age peaks.

silica-cemented supermature quartz arenite with syntaxial overgrowths (James & Oaks, 1977; Oaks et al., 1977). Many of the quartz grains present in the Kootenai Formation sandstones have syntaxial overgrowths; however, pore spaces are commonly filled by pseudomatrix (deformed mudstone lithics), carbonate cement, and to a lesser degree silica cement (Figures 5b and 5c). We interpret that these overgrowths are more indicative of the source strata rather than pervasive, in situ silica cementation in Lower Cretaceous strata. Chert and quartzite pebbles within the basal conglomerate and chert and mudstone lithics in the sandstones of the Kootenai Formation can also be attributed to lower-middle Paleozoic strata in central Idaho. In particular, the Devonian Milligen Formation (Ross, 1934; Umpleby et al., 1930) contains shale, siltstone, chert, impure limestone, limy shale, and fossiliferous limestone with chert interbeds. Furthermore, the Mississippian Copper Basin Group contains conglomerates and deep marine turbidites that are composed of argillites, quartzites, and cherts (Link et al., 1996; Nilsen, 1977).

5.5. Type III Provenance—Hinterland Plutons

Previous workers in northwestern Montana and southern Alberta interpreted a plutonic source for sandstones that we classify as Type III based on abundant biotite (Walker, 1974) and volcanic lithics (Gillespie, 1992; Rapson, 1964, 1965). Based on work on rocks exposed between Calgary, Alberta, and Fernie, British Columbia, Rapson (1964, 1965) suggested that some of those sandstones may have been sourced from west of the thrust belt in metamorphic and volcanic terranes of the Omineca and Intermontane belts; Gillespie (1992) identified the same potential source terranes. More recently, combined detrital zircon U-Pb geochronology and thin section analysis from the upper part of the Kootenai Formation revealed ages of 110–115, 160, and minor 190–220 Ma in addition to the presence of plagioclase feldspar and volcanic lithics in thin section (Fuentes et al., 2011; Quinn et al., 2018). Fuentes et al. (2011) interpreted source regions for these strata in the Omineca or Intermontane belts; specific source terranes were not identified by Quinn et al. (2018). Some workers have suggested that a more southerly position for these source terranes would be required for connections to have been feasible (e.g., Pană et al., 2019; Wyld et al., 2006).

We document the first occurrence of Type III sandstone in southwestern Montana, which is present at the Cinnabar Mountain locality (Figure 2). Through comparison with previously published data from sandstones that we classify as Type III, we find that this signature is dominated by Mesozoic ages (Figure 8). In particular, ~110–115 and ~160 Ma populations that are not present in the underlying Jurassic strata require a primary igneous or first-cycle source for these grains. Due to the high-precision, low-n data that is typically collected from igneous rocks, mixture modeling for the Type III composite is unreliable. Instead, the Type III regional composite signature was qualitatively compared with detrital zircon spectra from outboard potential source regions and Cretaceous strata that may have shared an igneous source with the foreland (Figure 11; Gaschnig et al., 2017; LaMaskin et al., 2011; Surpless et al., 2014).

The Blue Mountains province (Figure 1), which is currently at the latitude of the Idaho-Montana fold-thrust belt, represents a potential source region containing igneous plutons and older Mesozoic strata that may have been sources for the Type III sandstones. Plutons of the Blue Mountains province show four main pulses of magmatism from Middle Jurassic to Early Cretaceous time with ages of 154–162, 141–148, 123–129, and 111–124 Ma in addition to late Permian ages (Figure 11; Gaschnig et al., 2017; Kurz et al., 2012; Schwartz, Johnson, et al., 2011; Schwartz, Snoke, et al., 2011; Schwartz et al., 2014; Ware, 2013). Additionally, the older Mesozoic strata from that region, which may represent a potential recycled source (Figure 11), contain a broad age cluster that ranges from ~150 to 230 Ma with most ages occurring between 180 and 220 Ma (LaMaskin et al., 2011; Schwartz, Snoke, et al., 2011). In contrast, the Type III U-Pb regional composite signature from the Kootenai Formation contains age peaks at 112 and 162 Ma, tends to lack ages

between 123 and 148 Ma, and contains much less prominent age groups older than 180 Ma. If this region was a significant source area, we would expect a much broader cluster of ages, including Permian, Triassic, and Early Jurassic populations to be present in the Type III signature. Based on this comparison, we find that ages in the Type III detrital zircon signature are inconsistent with a dominantly Blue Mountains provenance (Figure 11).

The Eagle Plutonic complex, which is near the boundary between the Insular and Intermontane terranes (Figure 1), contains a ~148–157 Ma group of plutons that are crosscut by the ~111 Ma Fallslake Plutonic Suite (Greig et al., 1992). This plutonic complex has previously been interpreted as the main source for Cretaceous strata in the Methow basin, which was likely in a forearc position relative to its potential source area prior to ~100 Ma (Hurlow, 1993). Consistent with the Type III regional composite, detrital zircon data from the Methow basin (Figure 1) display a remarkably uniform detrital zircon signature with age peaks at 115 and 160 Ma (Figure 11; Surpless et al., 2014). Although detrital zircon U-Pb age signatures are similar, this potential source area may have been too far west to be a dominant source for the Type III sandstones.

The Omineca belt, the southern extent of which is currently located ~400 km to the north of the study area, represents another potential source region (Figure 1). Along its southeastern edge, near Nelson, British Columbia, there is a plutonic suite with ages that range from ~156 to 172 Ma (Archibald et al., 1983; Carr, 1991; Ghosh, 1995; Sevigny & Parrish, 1993), which is crosscut by the ~117 Ma Baldy pluton (Webster et al., 2017). Comparison of those U-Pb ages with detrital zircon age peaks at 112 and 162 Ma in the Type III sandstones reveals notable overlap (Figure 11). Additionally, the >250 Ma age fraction of the Type III regional composite (Figure 9) contains a strong age peak at ca. 1,780 Ma, which is broadly consistent with mapped Cambrian and Neoproterozoic strata surrounding the Nelson batholith (Figure 1) and 1.7–2.0 Ga detrital zircon grains from metasedimentary strata in that region (Matthews et al., 2018; Ross & Parrish, 1991; Webster et al., 2017). Based on this comparison, we find that ages in the Type III detrital zircon signature are broadly consistent with igneous ages from plutons that intruded Cambrian and Neoproterozoic strata of the southern Omineca belt.

6. Discussion

6.1. Sediment Dispersal Model

Previous provenance analysis of Lower Cretaceous strata in western North America has been used to interpret a paleo-drainage divide in the Montana region (Leier & Gehrels, 2011). In the Canadian sector of the foreland, detrital zircon ages of ca. 120 and 1,850 Ma have been documented, whereas ages of ca. 160, 250–650, and 1,040 Ma occur in the southwestern United States and central Montana (Leier & Gehrels, 2011). Our study area in southwestern Montana represents a transitional area between these different provenance regions. For our sediment dispersal model, we utilize the concepts of transverse and axial drainage systems presented by Burbank (1992) and employed by Raines et al. (2013) to better understand regional paleodrainage networks. In general, transverse drainages (oriented perpendicular to the basin-axis) will flow from a thrust belt until they intersect an axial system (oriented parallel to the basin-axis). During times of increased tectonic loading, transverse and axial systems are confined to regions near the thrust belt and during times of tectonic quiescence, erosional unloading, and rebound, the river systems migrate to a more distal position relative to the thrust belt (e.g., Heller et al., 1988).

6.1.1. Stage 1—Berrasian(?)-Aptian (145–112 Ma)

A previous sediment dispersal model, based on paleocurrent analysis and detrital zircon samples from Great Falls, MT, interprets a north-flowing axial system with potential headwaters located in the southwestern U.S. (Quinn et al., 2018). Our findings are consistent with that model and help to refine it because our new detrital zircon data present the possibility that an axial system passed through southwestern Montana prior to reaching Great Falls. In our model, coeval sediment dispersal of Type I and II sandstones occurred during deposition of the Lower clastic member of the Kootenai Formation by a combination of axial and transverse drainages that had headwaters in distinct source areas (Figure 12a). Combined paleocurrent, petrographic, and detrital zircon analysis suggests that Type I quartz-rich sediment was mainly transported via an axial fluvial system that connected an exhumed Jurassic aeolianite source within and north of the Colorado Plateau highland region with western and central Montana (Quinn et al., 2018). Evidence for an axial system

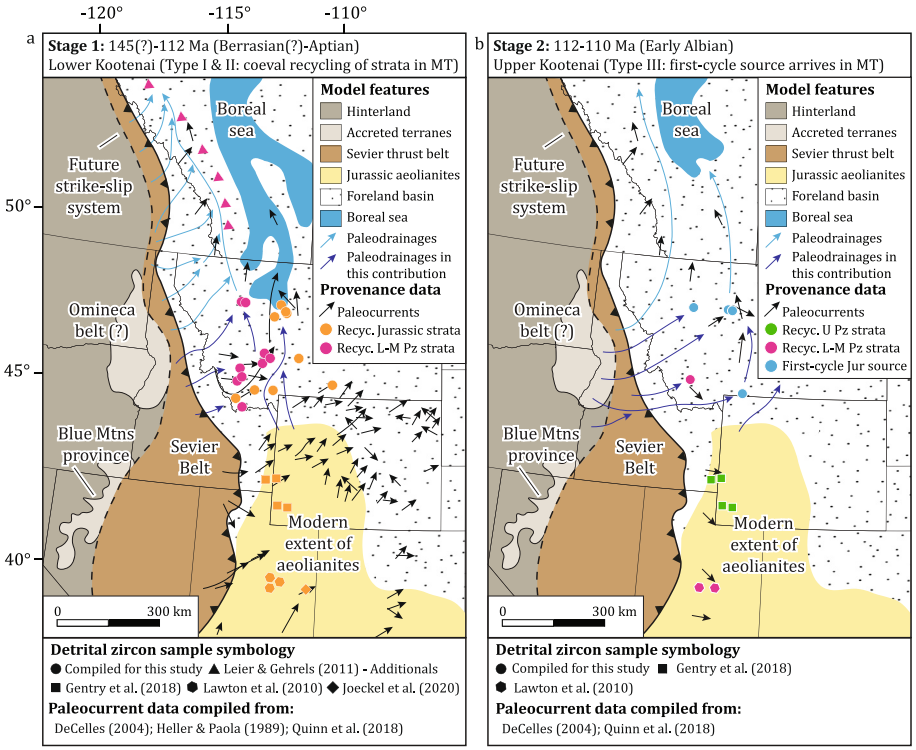

Figure 12. Schematic sediment dispersal model for deposition of Lower Cretaceous strata in western North America; dark blue arrows represent interpreted paleodrainages in this contribution. (a) Stage 1: model for sediment dispersal during deposition of the Lower Kootenai Formation. (b) Stage 2: model for sediment dispersal during deposition of the Upper Kootenai Formation (coordinates displayed as NAD83; model features adapted from: Blum & Pecha, 2014—Early Albian paleodrainage systems depicted as light blue arrows; DeCelles, 2004—paleocurrents; Dickinson & Gehrels, 2009a—modern extent of Jurassic aeolianites; Dorsey & LaMaskin, 2007—Early Cretaceous location of Blue Mountains province; Gentry et al., 2018—detrital zircon samples in southern Idaho and Wyoming; Heller & Paola, 1989—paleocurrents; Horner et al., 2019—Aptian paleodrainage systems depicted as light blue arrows; Joeckel et al., 2020—detrital zircon sample in eastern Utah; Lawton et al., 2010—detrital zircon samples in Utah; Leier & Gehrels, 2011—detrital zircon samples in Canada; Quinn et al., 2018—paleocurrents; Schwartz & DeCelles, 1988—foreland basin; Schwartz & Vuke, 2019—Boreal sea; Wright & Wyld, 2007—Blue Mountains province position and shear zone; Wyld et al., 2006—shape of Omineca belt; Yonkee & Weil, 2015—thrust front).

stems from the presence of these highlands in the southwestern U.S. and previous work in the Great Falls region (Figure 2; Quinn et al., 2018). In Great Falls, paleocurrent analysis from the nonmarine Cutbank member indicates north- and northeast-directed paleoflow, whereas the marginal marine Sunburst member contains a ~220-m wide, ~24-m deep north-trending channel with west-directed paleocurrent indicators (Hopkins, 1985; Quinn et al., 2018; Schwartz & Vuke, 2019; Walker, 1974). In our model, this potential axial system may have been located between the Ruby River and Lincoln Mountain or Taylor Fork Creek localities (Figures 2 and 12a), where a >50 m thick accumulation of cross-bedded sandstone and gravel is exposed within the Gravelly Range (DeCelles, 1986).

To the west of the Great Falls axial system, Type II sandstone was delivered to the southwestern Montana foreland by transverse sediment dispersal systems that drained lithic-rich, lower-middle Paleozoic strata from the active thrust front in east-central Idaho, resulting in westerly derived fluvial sedimentary cover throughout western Montana (Figure 12a). Thrusting, possibly along the Pioneer thrust fault (Figure 1), likely occurred during this time based on subsidence analysis (Fuentes et al., 2011). Within this context, we interpret that transverse systems were likely short and the axial system was relatively close to the thrust belt (e.g., Burbank, 1992; Heller et al., 1988; Raines et al., 2013). The basis for dispersal from the west stems from outcrop and thin section analysis by numerous workers throughout western Montana (e.g., DeCelles, 1986; Fuentes et al., 2011; Suttner et al., 1981). In southwestern Montana, compiled data suggest mainly east-directed paleocurrent indicators (e.g., DeCelles, 2004; Heller & Paola, 1989), chert-rich sandstones derived

from the thrust belt (DeCelles, 1986), and new detrital zircon provenance data that match very well with exhumed lower-middle Paleozoic passive margin strata. Based on our mixture modeling of the Type II regional composite detrital zircon signature (Figure 10b), >60% of the detrital zircon grains in Type II sandstone were recycled from Ordovician, Devonian, and Mississippian strata. Transverse drainages are strongly supported by detrital zircon provenance because lower-middle Paleozoic clastic rocks are not present in southwestern Montana, yet they are common to the west in Idaho. Additionally, the relatively few ~110–115 Ma detrital zircon grains in the lower intervals of the Kootenai Formation could have been derived from air-fall events, but most zircon grains were subsequently redistributed by fluvial systems. Potential arc sources for air-fall zircons include the older, missing segments of the Idaho batholith, the Omineca belt, and the Coast Mountains batholith. The more distal Sierra Nevada arc system was not especially active during ~115–110 Ma (Ducea, 2001). Toward the end of this interval, coarse clastic sedimentation ceased and local lacustrine systems developed based on deposition of the Lower calcareous member (Figure 4).

6.1.2. Stage 2—Early Albian (112–110 Ma)

During deposition of the Upper clastic member of the Kootenai Formation (Figures 4 and 12b), it is likely that dispersal of Type I sandstones by axial drainages continued, but perhaps the system migrated eastward toward central Montana because the Type I signature has not been documented in sandstones of this age in southwestern Montana. The key difference during this stage is the arrival of Type III sandstones to the western Montana foreland (Fuentes et al., 2009; Quinn et al., 2018; this study). Based on evaluation of our new detrital zircon data within the context of previous work, we interpret that Type II and III sandstones were both delivered to the foreland during this stage by transverse drainages. The main evidence for transverse drainages is based on provenance analysis of the Type II and III sandstones, both of which we attribute to western sources. The basis for the Type II western source was described in the first stage of the model; the Type III western source is based on the abundant ~160 Ma detrital zircon grains in those samples and east-directed paleocurrent indicators in the Upper Kootenai member (Figure 3; Fifth member) near Great Falls, MT (Quinn et al., 2018). The underlying Red sandstone from that region records north-directed dispersal (Quinn et al., 2018); however, as demonstrated by Thomas (2011), some paleocurrent data may be inconsistent with the overall trend of a river system, especially when meandering has occurred. Therefore, during this time, we interpret that river systems were generally less confined to the region near the thrust belt and were able to expand their reach across southwestern Montana (e.g., Burbank, 1992). In our model, the Type III sandstones were transported to the basin by fluvial systems with headwaters in the hinterland of the orogen (Figure 12b). These fluvial systems likely incised into and drained an ~160 Ma plutonic suite, which may have been overlain by an ~110–115 Ma volcanic carapace. Alternatively, the ~110–115 Ma detrital zircon grains could have been contributed by air-fall events emanating from older, missing segments of the Idaho batholith, the Omineca belt, and the Coast Mountains batholith. Lastly, toward the end of this interval, coarse clastic sedimentation once again ceased and widespread lacustrine systems developed as recorded by the Upper calcareous member (Figure 4).

6.2. Regional Tectonic Significance for the Provenance of the Kootenai Formation

6.2.1. Subtle Tectonic Partitioning in the Southwestern Montana Foreland During Early Cretaceous Time

Our study area includes a region of basement-involved thrusting that defines the northwestern edge of the Laramide structural province (Figure 1). Based on the Mesozoic sedimentary record in this area, previous workers have interpreted a long history (~100 Myr) of basement-involved deformation that includes minor tilting and erosion during Jurassic time (Schwartz & DeCelles, 1988), followed by subtle tectonic partitioning in southwestern Montana during Early Cretaceous time (Carrapa et al., 2019; DeCelles, 1986). This partitioning history is markedly older than foreland basin partitioning elsewhere in the Laramide province, most of which occurred after 80 Ma (e.g., Copeland et al., 2017). One of the broader goals of our project is to better understand the timing of basement-involved deformation during Mesozoic orogenesis in the Idaho-Montana sector of the orogen; for this study, our approach is to use U-Pb detrital zircon data in an attempt to better constrain the timing of basin partitioning events.

Our provenance analysis indicates sources for the Kootenai Formation that are mainly older strata and igneous rocks located beyond the basin, rather than local strata in southwestern Montana, suggesting a dominantly extrabasinal provenance. The findings of our study do not preclude subtle Early Cretaceous partitioning interpreted by previous workers in the southwestern Montana foreland (DeCelles, 1986); however, our results reinforce the concept that partitioning in this region during Early Cretaceous time was not of the same magnitude as traditionally defined Laramide-style partitioning—which includes development of local depocenters adjacent to basement-cored uplifts that contain wholesale recycling of strata from the tops of basement arches (e.g., Horton et al., 2016; Lawton, 2019). Additionally, our findings provide new timing constraints for the interpretations of previous workers, who have suggested an early (pre-Late Cretaceous?) episode of low magnitude, basement-involved thrusting in southwestern Montana and east-central Idaho (Perry et al., 1983); perhaps more significant basement-involved deformation occurred both prior to and after the deposition of the Kootenai Formation as recorded by the ~10° angular unconformity between Upper Jurassic and Lower Cretaceous strata and the Late Cretaceous conglomerates near the Blacktail-Snowcrest uplift (Figure 2; DeCelles, 1986, Garber et al., 2020; Mann, 1954). Despite any subtle, localized tectonic partitioning during Early Cretaceous time, our analysis is consistent with river systems that remained connected and through-flowing from the fold-thrust belt to the Boreal Sea in Canada.

6.2.2. Moderate Strike-Slip Displacement Along the Western Idaho Shear Zone?

An important and unresolved Early Cretaceous controversy surrounds the translational history and paleography of the accreted Cordilleran terranes. One model, referred to as the Baja British Columbia hypothesis, which is largely based on paleomagnetism, suggests that the Insular and Intermontane superterranes—in addition to the western portion of the Coast Mountains batholith—may have docked upto 3,000 km to the south of their current positions (Butler et al., 2001; Cowan et al., 1997; Enkin, 2006). Other models, however, which are based on constraints such as magmatic ages, metamorphism, restoration of strike-slip faults, or provenance of strata have led workers to suggest that those terranes may not be as far-traveled (e.g., DeGraff-Surpless et al., 2003; Gehrels et al., 2009; Wyld et al., 2006). Furthermore, there were likely components of both dextral and sinistral translation throughout their accretionary histories (Chardon et al., 1999; Enkin, 2006; Gehrels et al., 2009). Wyld et al. (2006) presented a middle Cretaceous (100 Ma) paleogeographic reconstruction for the North American Cordillera based on restoration of Late Cretaceous to Cenozoic contractional and extensional belts, and dextral strike-slip systems. When restored, some of the easternmost outboard terranes, including the Blue Mountains province, portions of the southern Omineca belt, and the Methow–Tyaughton basin are juxtaposed with western Idaho and partly fill in the Columbia embayment. In a later reconstruction by Wright and Wyld (2007), consistent with that of Dorsey and LaMaskin (2007), the Blue Mountains province is juxtaposed with western Nevada. Wyld et al. (2006) suggested that if their paleogeographic reconstruction is valid, geologic features of the terranes should match with those on the *in situ* portion of the continent.

We propose that the Kootenai Formation provenance data set may be a reasonable test of paleogeographic reconstructions such as that of Wyld et al. (2006). This formation was deposited on the *in situ* portion of the Cordillera during Early Cretaceous time and contains sandstones that are dominated by ~160 Ma detrital zircon ages with interpreted sources in the hinterland of the orogen that were dislocated by transcurrent fault systems. Our provenance interpretations provide support for paleogeographic reconstructions in which Jurassic plutons of the southern Omineca belt are a source for the Type III sandstones of the Kootenai Formation. Similar to the reconstruction by Wyld et al. (2006), other workers suggest that extensional structures in the southern Omineca belt may have been kinematically linked with nearby strike-slip faults prior to Late Cretaceous time (e.g., McClelland et al., 2000; van der Velon & Cook, 1996). In addition, prior to overprinting by Eocene extension in the southern Omineca belt, there may have been a major through-going strike-slip fault in this region (Irving et al., 1996; McClelland & Oldow, 2007). Identification of connections between the retroarc portion of the system and southern portions of the Intermontane superterrane during this time is not a new finding (Fuentes et al., 2011; Gillespie, 1992; Quinn et al., 2016, 2018; Walker, 1974); however, prior to our study, a connection had not been recognized in southwestern Montana. Based on this, one possibility is that at the latitude of our study area (44°–48°N) during Aptian-Albian time, portions of the southern Omineca belt were located west of the Idaho-Montana region, in the vicinity of where the Blue Mountains province is situated today (Figure 12).

6.3. Broader Tectonic Significance for the Provenance of the Kootenai Formation

6.3.1. Provenance Comparison of Lower Cretaceous Synorogenic Strata Across the North American Cordilleran Foreland Basin System

Previous detrital zircon provenance analysis of Early Cretaceous synorogenic strata in the North American Cordilleran foreland basin system has been used to interpret differential exposure of source strata in the Sevier fold-thrust belt (Leier & Gehrels, 2011). The new provenance data from the Kootenai Formation presented in this study are from a transitional region between the Canadian and southwestern U.S. sectors of the foreland basin system, where northern (ca. 1,850 Ma ages) and southern (ca. 1,040 Ma ages) detrital zircon signatures have been documented in Lower Cretaceous strata (Leier & Gehrels, 2011; Raines et al., 2013). Provenance of the Kootenai Formation in southwestern Montana is consistent with both signatures; we interpret that the northern signature reflects transverse fluvial systems, whereas the southern signature reflects an axial fluvial system. Prior to this study, the northern signature had not been documented as far south as southwestern Montana.

Comparison of detrital zircon data from Aptian strata of western Montana with samples from Alberta, Idaho, Wyoming, and Utah (Gentry et al., 2018; Lawton et al., 2010; Raines et al., 2013), documents two main signatures (our Types I and II); however, there is a change in provenance near southwestern Montana marked by the presence of the Type II samples (Figure 12a). In contrast, early Albian data from that same region are more sparse but reveal a more complicated provenance including upper Paleozoic source strata in southern Idaho and first-cycle sources from the hinterland of the system in western Montana (Figure 12b). Based on our comparison of Early Cretaceous provenance data across the foreland, perhaps there was a discontinuity in exposed source strata near southwestern Montana, or a general northward progression in which exhumation and erosion of deeper source strata occurred to the north of southwestern Montana. In southern Idaho, Wyoming, and central Utah, source strata in the thrust belt may have been less deeply exhumed during Early Cretaceous time.

6.3.2. Sedimentation During the Initial Stages of North American Cordilleran Foreland Basin Development

A significant finding of our provenance analysis is that lower Mesozoic and upper Paleozoic strata were not identified as primary sources for the Kootenai Formation in southwestern Montana based on visual analysis of detrital zircon U-Pb age spectra or mixture modeling (Triassic & Pennsylvanian-Permian; Figures 9 and 10). Rather, the source for the bulk of the of Kootenai Formation in our study area is interpreted as lower-middle Paleozoic (Ord-Dev-Miss) strata, which requires pre-Kootenai Formation tectonism in the Idaho-Montana region. This tectonism likely included unroofing of lower Mesozoic and upper Paleozoic strata prior to deposition of the Kootenai Formation. One possible explanation is that the missing upper Paleozoic detritus may have accumulated in an Early Cretaceous western Montana phantom foredeep, like the case in west-central Utah (Fuentes et al., 2011; Royse, 1993); however, this volume of sediment was not subsequently recycled and transported eastward into the distal portion of the foredeep based on our provenance analysis. Another possibility is that upper Paleozoic sediments were not retained in the proximal portions of the foredeep in western Montana (e.g., Heller et al., 2003); instead, those sediments bypassed the region during or prior to development of the sub-Cretaceous unconformity and were transported to the north in Alberta, where they were retained in a separate sector of the Late Jurassic-Early Cretaceous foreland (e.g., Pană et al., 2019). Evidence for this interpretation stems from the provenance analysis of Raines et al. (2013): they call upon an anomalous southern axial source for detrital zircon grains from the Late Jurassic-Early Cretaceous Monteith and Nikanassin formations that display a broad range of ca. 980–2,000 Ma ages—perhaps this source was lower Mesozoic and upper Paleozoic strata that were shed from the Idaho-Montana sector of the Sevier belt during pre-Kootenai Formation tectonism.

6.3.3. Evaluation of Kootenai Formation Provenance Data Within the Context of Competing Models for Foreland Basin Sedimentation

In general, there are two competing models for foreland basin sedimentation. The traditional model suggests coarse-grained detritus overwhelms the entire foredeep during pulses of tectonism; in this model, fine-grained strata that are deposited in the distal foredeep reflect tectonic quiescence (e.g., Haque et al., 2020). In contrast, a two-stage model suggests that during pulses of tectonism, coarse-grained strata are confined

to the proximal foredeep and fine-grained strata are deposited in the distal foredeep; in this alternative model, isostatic rebound of the orogenic system results in deposition of coarse-grained strata in the distal foredeep (e.g., Heller et al., 1988). The Kootenai Formation in southwestern Montana is reflective of sedimentation in the distal foredeep and contains a succession of clastic strata with intervening fine-grained carbonate units (Figure 4); improved age control on the fine-grained units may help to better understand sedimentation during the early stages of foreland basin development (e.g., Finzel & Rosenblume, 2021).

Although this study did not focus on the fine-grained units of the Kootenai Formation, evaluation of our new provenance data within the context of these foreland basin sedimentation models reveals a few useful insights. One noteworthy finding is the difference in provenance within the Type II samples between the Lower clastic and Upper clastic members at the Ziegler Gulch locality (Figures 2 and 7). All detrital zircon data from the Lower clastic member contain sparse near-depositional age grains and a relatively minor ca. 1,780 Ma age peak when compared with the Upper clastic member (Figure 7; ZG-186m). Evaluation of this difference within the context of the traditional model would suggest that detrital zircon ages from the Upper clastic member sample (Figure 7; ZG-186m) are reflective of both increased magmatism and thrusting based on the introduction of ca. 112 Ma ages and the more well-developed ca. 1,780 Ma age peak that resembles the Cambrian rather than Ord-Dev-Miss source strata composite detrital zircon signature (Figure 9). In the context of the two-stage model, however, near-depositional age detrital zircon grains have also been recovered from the intervening limestone units, suggesting air-fall volcanism occurred during deposition of those units—the possibility remains that they may represent the earliest onset of subsidence, rather than tectonic quiescence, in the distal foredeep (e.g., Finzel & Rosenblume, 2021).

7. Conclusions

The Lower Cretaceous Kootenai Formation in southwestern Montana holds a record of initial sedimentation in the distal foredeep of the North American Cordilleran foreland basin system. The new data presented herein fill a notable gap in the Idaho-Montana sector of the Early Cretaceous foreland basin system. In this study, we use sandstone petrography, large-n ($n = 600$) detrital zircon geochronology, and provenance mixture modeling to determine three primary sources for the Kootenai Formation. Based on our provenance analysis, the three sources are (1) recycled Jurassic continental strata located to the south of the study area, (2) recycled lower-middle Paleozoic strata in central Idaho exhumed by the Sevier fold-thrust belt, and (3) hinterland sources containing ~160 Ma plutons that were subsequently dislocated along margin-parallel transcurrent faults.

We present a new sediment dispersal model for the southwestern Montana foreland basin that incorporates axial drainages with headwaters to the south of the study area, possibly as far as the Colorado Plateau highlands and transverse drainages with headwaters to the west of the study area in the Idaho sector of the Sevier fold-thrust belt. In our model, during Barremian(?)-Aptian time, axial drainages, which carried recycled Jurassic sediments from the Colorado Plateau region, passed through southwestern Montana as they flowed north toward the Boreal Sea in Canada. In contrast, transverse drainages carried lithic-rich lower-middle Paleozoic sediment to the western Montana foreland, where they may have mixed with southern-sourced sediments. During Early Albian time, first-cycle sediment was transported to the western Montana foreland by transverse drainages with headwaters in the hinterland of the orogen.

Regional tectonic implications of our provenance analysis are two-fold. First, the extrabasinal sources for the Kootenai Formation reinforce the concept that subtle, localized tectonic partitioning during Early Cretaceous time in southwestern Montana was limited and only generated minor, highly localized structural relief. Some of this structural relief could also be related to the passage of an irregular flexural forebulge (Carrapa et al., 2019). Second, the strong ca. 160 Ma detrital zircon age peak in sandstones from the uppermost Kootenai Formation document a connection between the hinterland and the foreland of the orogen; this connection establishes potential linkages with outboard terranes.

Broader tectonic implications of our provenance analysis are three-fold. First, a comparison of Lower Cretaceous provenance across the foreland from Utah to Alberta suggests either a discontinuity in the unroofing level of source strata near southwestern Montana or a general northward progression of the system from more shallow unroofing in Utah toward deeper unroofing of source strata in Alberta. Second, the bulk of

the provenance data from the Kootenai Formation in southwestern Montana lacks notable contributions from lower Mesozoic and upper Paleozoic source strata, which requires exhumation of the fold-thrust belt prior to deposition of the Kootenai Formation. Last, comparison with both the traditional and two-stage models for foreland basin sedimentation suggests detailed geochronological work is needed to better understand the timing of basin-wide subsidence events.

Data Availability Statement

Data supporting the conclusions are available in the supporting information and at https://www.geochron.org/detritalsearch.php by navigating to southwestern Montana on the map interface.

Acknowledgments
This study represents a portion of J. A. Rosenblume's Ph.D. thesis. J. A. Rosenblume and E. S. Finzel thank University of Iowa students Benjamin Howard, Alethea Kapolas, and Cole Gardner for assistance with field work and sample analysis. Thanks to Mark Pecha, Kurt Sundell, and Sarah George for support at the Arizona Laserchron Center. J. A. Rosenblume thanks W.C. McClelland for thought-provoking discussions and Larissa da Rocha Santos for assistance with GIS. This manuscript was greatly improved by suggestions from Majie Fan, Andrew Leier, and an anonymous reviewer. Funding for this research was provided by NSF-Tectonics EAR-1727504 (Finzel) and EAR-1728563 (Pearson), NSF EAR-1649254 (Arizona LaserChron Center), and graduate student awards to J.R. from the Tobacco Root Geological Society and the University of Iowa EES Department's Sullivan-Smith, Furnish-Glenister, and Leisch Funds.

References

Archibald, D. A., Glover, J. K., Price, R. A., Farrar, E., & Carmichael, D. M. (1983). Geochronology and tectonic implications of magmatism and metamorphism, southern Kootenay Arc and neighboring regions, southeastern British Columbia. Part I: Jurassic to mid-Cretaceous. *Canadian Journal of Earth Sciences*, *20*, 1891–1913. https://doi.org/10.1139/e83-178

Baar, E. E. (2009). *Determining the regional-scale detrital zircon provenance of the middle-late Ordovician Kinnikinic (Eureka) quartzite, east-central Idaho, U.S.* (pp. 134). Pullman, WA: Washington State University. M.S. thesis.

Ballard, W. W. (1966). Petrography of Jurassic and Cretaceous sandstones north flank Little Belt Mountains, Montana. In J. E. Cox, L. E. Hunter, & J. E. Blair (Eds.), *17th annual field conference guidebook: Great Falls, Montana* (pp. 56–70). Billings Geological Society.

Benyon, C., Leier, A., Leckie, D. A., Webb, A., Hubbard, S. M., & Gehrels, G. (2014). Provenance of the Cretaceous Athabasca Oil Sands, Canada: Implications for continental-scale sediment transport. *Journal of Sedimentary Research*, *84*, 136–143. http://dx.doi.org/10.2110/jsr.2014.16

Benyon, C., Leier, A. L., Leckie, D. A., Hubbard, S. M., & Gehrels, G. E. (2016). Sandstone provenance and insights into the paleogeography of the McMurray Formation from detrital zircon geochronology, Athabasca Oil Sands, Canada. *AAPG Bulletin*, *100*(2), 269–287. https://doi.org/10.1306/10191515029

Beranek, L. P., Link, P. K., & Fanning, C. M. (2016). Detrital zircon record of mid-Paleozoic convergent margin activity in the northern U.S. Rocky Mountains: Implications for the Antler orogeny and early evolution of the North American Cordillera. *Lithosphere*, *8*(5), 533–550. https://doi.org/10.1130/L557.1

Berg, R. B., Lonn, J. D., & Locke, W. W. (1999). *Geologic map of the Gardiner 30' × 60' Quadrangle, south-central Montana*. Montana Bureau of Mines and Geology. Open-File Reports MBMG-387, 1 sheet, scale 1:100,000.

Blum, M., & Pecha, M. (2014). Mid-Cretaceous to Paleocene North American drainage reorganization from detrital zircons. *Geology*, *42*(7), 607–610. https://doi.org/10.1130/G35513.1

Brennan, D. T., Pearson, D. M., Link, P. K., & Chamberlain, K. R. (2020). Neoproterozoic Windermere Supergroup near Bayhorse, Idaho: Late-stage Rodinian rifting was deflected west around the Belt basin. *Tectonics*, *39*, e2020TC006145. https://doi.org/10.1029/2020TC006145

Brown, E. H., & Gehrels, G. E. (2007). Detrital zircon constraints on terrane ages and affinities and timing of orogenic events in the San Juan Islands and North Cascades, Washington. *Canadian Journal of Earth Sciences*, *44*, 1375–1396. https://doi.org/10.1139/e07-040

Burbank, D. W. (1992). Causes of recent Himalayan uplift deduced from deposited patterns in the Ganges basin. *Nature*, *357*, 680–683. https://doi.org/10.1038/357680a0

Burden, E. T. (1984). Terrestrial palynomorph biostratigraphy of the lower part of the Mannville Group (Lower Cretaceous), Alberta and Montana. In D. F. Stott, & D. J. Glass (Eds.), *The Mesozoic of Middle North America, Canadian Society of Petroleum Geologists Memoir 9* (pp. 249–269). Canadian Society of Petroleum Geologists.

Butler, R. F., Gehrels, G. E., & Kodama, K. P. (2001). A moderate translation alternative to the Baja British Columbia Hypothesis. *Geological Society of America Today*, *11*(6), 4–10. https://doi.org/10.1130/1052-5173(2001)011<0004:amtatt>2.0.co;2

Carrapa, B., DeCelles, P. G., & Romero, M. (2019). Early Inception of the Laramide Orogeny in Southwestern Montana and Northern Wyoming: Implications for models of flat-slab subduction. *Journal of Geophysical Research: Solid Earth*, *124*, 2102–2123. https://doi.org/10.1029/2018JB016888

Carr, S. D. (1991). U-Pb zircon and titanite ages of three Mesozoic igneous rocks south of the Thor-Odin – Pinnacles area, southern Omineca Belt, British Columbia. *Canadian Journal of Earth Sciences*, *28*, 1877–1882. https://doi.org/10.1139/e91-168

Chardon, D., Andronicos, C. L., & Hollister, L. S. (1999). Large-scale transpressive shear zone patterns and displacements within magmatic arcs: The Coast Plutonic Complex, British Columbia. *Tectonics*, *18*(2), 278–292. https://doi.org/10.1029/1998TC900035

Cobban, W. A. (1955). Cretaceous Rocks of Northwestern Montana. In *6th annual field conference guidebook* (pp. 107–119). Billings, MT: Billings Geological Society.

Coney, P. J., & Evenchick, C. A. (1994). Consolidation of the American Cordilleras. *Journal of South American Earth Sciences*, *7*(3–4), 241–262. https://doi.org/10.1016/0895-9811(94)90011-6

Copeland, P., Currie, C. A., Lawton, T. F., & Murphy, M. A. (2017). Location, location, location: The variable lifespan of the Laramide orogeny. *Geology*, *45*(3), 223–226. https://doi.org/10.1130/G38810.1

Coutts, D. S., Matthews, W. A., & Hubbard, S. M. (2019). Assessment of widely used methods to derive depositional ages from detrital zircon populations. *Geoscience Frontiers*, *10*, 1421–1435. https://doi.org/10.1016/j.gsf.2018.11.002

Cowan, D. S., Brandon, M. T., & Garver, J. I. (1997). Geological tests of hypotheses for large coastwise displacements; a critique illustrated by the Baja British Columbia controversy. *American Journal of Science*, *297*, 117–173. https://doi.org/10.2475/ajs.297.2.117

DeCelles, P. G. (1984). *Sedimentation and diagenesis in a tectonically partitioned, nonmarine foreland basin: The Lower Cretaceous Kootenai Formation, southwestern Montana* (pp. 423). Bloomington, IN: Indiana University. Ph.D. thesis.

DeCelles, P. G. (1986). Sedimentation in a tectonically partitioned, nonmarine foreland basin: The Lower Cretaceous Kootenai Formation, southwestern Montana. *The Geological Society of America Bulletin*, *97*, 911–931. https://doi.org/10.1130/0016-7606(1986)97<911:siatpn>2.0.co;2

DeCelles, P. G. (2004). Late Jurassic to Eocene evolution of the Cordilleran thrust belt and foreland basin system, Western U.S.A. *American Journal of Science*, *304*, 105–168. https://doi.org/10.2475/ajs.304.2.105

DeCelles, P. G. (2012). Foreland basin systems revisited: Variations in response to tectonic settings. In C. Busby, & A. Azor Perez (Eds.), *Tectonics of sedimentary basins: Recent advances* (1st ed., pp. 405–426). Blackwell Publishing Ltd.
DeCelles, P. G., & Giles, K. A. (1996). Foreland basin systems. *Basin Research*, *8*, 105–123. https://doi.org/10.1046/j.1365-2117.1996.01491.x
DeCelles, P. G., Pile, H. T., & Coogan, J. C. (1993). Kinematic history of the Meade thrust based on provenance of the Bechler conglomerate at Red Mountain, Idaho, Sevier thrust belt. *Tectonics*, *12*(6), 1436–1450. https://doi.org/10.1029/93tc01790
DeGraff-Surpless, K., Mahoney, J. B., Wooden, J. L., & McWilliams, M. O. (2003). Lithofacies control in detrital zircon provenance studies: Insights from the Cretaceous Methow basin, southern Canadian Cordillera. *The Geological Society of America Bulletin*, *115*(8), 899–915.
Dickinson, W. R. (2004). Evolution of the North American Cordillera. *Annual Review of Earth and Planetary Sciences*, *32*, 13–45. https://doi.org/10.1146/annurev.earth.32.101802.120257
Dickinson, W. R., & Gehrels, G. E. (2008). Sediment delivery to the Cordilleran foreland basin: Insights from U-Pb ages of detrital zircons in Upper Jurassic and Cretaceous strata from the Colorado Plateau. *American Journal of Science*, *308*, 1041–1082. https://doi.org/10.2475/10.2008.01
Dickinson, W. R., & Gehrels, G. E. (2009a). U-Pb ages of detrital zircons in Jurassic eolian and associated sandstones of the Colorado Plateau: Evidence for transcontinental dispersal and intraregional recycling of sediment. *The Geological Society of America Bulletin*, *121*(3–4), 408–433. https://doi.org/10.1130/B26406.1
Dickinson, W. R., & Gehrels, G. E. (2009b). Use of U-Pb ages of detrital zircons to infer maximum depositional ages of strata: A test against a Colorado Plateau Mesozoic database. *Earth and Planetary Science Letters*, *288*, 115–125. https://doi.org/10.1016/j.epsl.2009.09.013
Dickinson, W. R., & Snyder, W. S. (1978). Plate tectonics of the Laramide orogeny. In V. Matthews (Ed.), Laramide folding associated with basement block faulting in the western United States, Geological Society of America Memoir (Vol. 151, pp. 355–366). Denver, CO: Geological Society of America.
Dolson, J. C., & Piombino, J. (1994). Giant proximal foreland basin non-marine wedge trap: Lower Cretaceous Cutbank Sandstone, Montana. In J. C. Dolson, M. L. Hendricks, & W. A. Wescott (Eds.), *Unconformity-related hydrocarbons in sedimentary sequences, Rocky Mountain Association of Geologists Guidebook* (pp. 135–148). Rocky Mountain Association of Geologists.
Dorsey, R. J., & LaMaskin, T. A. (2007). Stratigraphic record of Triassic-Jurassic collisional tectonics in the Blue Mountains Province, Northeastern Oregon. *American Journal of Science*, *307*, 1167–1193. https://doi.org/10.2475/10.2007.03
Dover, J. H. (1980). Status of the Antler orogeny in central Idaho – clarifications and constraints from the Pioneer Mountains. In T. D. Fouch, & E. R. Magathan (Eds.), *Paleozoic Paleogeography of west-central United States, West-central United States paleogeography symposium 1* (pp. 371–386). Denver, CO: SEPM Rocky Mountain Section.
Ducea, M. (2001). The California Arc: Thick granitic batholiths, eclogitic residues, lithospheric-scale thrusting, and magmatic flare-ups. *Geological Society of America Today*, *11*, 4–10. https://doi.org/10.1130/1052-5173(2001)011<0004:tcatgb>2.0.co;2
Enkin, R. J. (2006). Paleomagnetism and the case for Baja British Columbia. In J. W. Haggart, R. J. Enkin, & J. W. H. Monger (Eds.), *Paleogeography of the North American Cordillera: Evidence for and against large-scale displacements: Geological Association of Canada, Special Paper 46* (pp. 233–253). Geological Association of Canada.
Finzel, E. S., & Rosenblume, J. A. (2021). Dating lacustrine carbonate strata with detrital zircon U-Pb geochronology. *Geology*, *49*. https://doi.org/10.1130/G48070.1
Foster, D. A., Mueller, P. A., Mogk, D. W., Wooden, J. L., & Vogl, J. J. (2006). Proterozoic evolution of the western margin of the Wyoming craton: Implications for the tectonic and magmatic evolution of the northern Rocky Mountains. *Canadian Journal of Earth Sciences*, *43*, 1601–1619. https://doi.org/10.1139/e06-052
Fox, R. D., & Groff, S. L. (1966). Stratigraphic and structural investigations of the Cascade-Ulm area, Montana. In J. E. Cox, L. E. Hunter, & J. E. Blair (Eds.), *17th annual field conference guidebook: Great Falls, Montana* (pp. 36–55). Billings Geological Society.
Fuentes, F., DeCelles, P. G., & Constenius, K. N. (2012). Regional structure and kinematic history of the Cordilleran fold-thrust belt in northwestern Montana, USA. *Geosphere*, *8*(5), 1104–1128. https://doi.org/10.1130/GES00773.1
Fuentes, F., DeCelles, P. G., Constenius, K. N., & Gehrels, G. E. (2011). Evolution of the Cordilleran foreland basin system in northwestern Montana, U.S.A. *The Geological Society of America Bulletin*, *123*(3–4), 507–533. https://doi.org/10.1130/B30204.1
Fuentes, F., DeCelles, P. G., & Gehrels, G. E. (2009). Jurassic onset of foreland basin deposition in northwestern Montana, USA: Implications for along-strike synchroneity of Cordilleran orogenic activity. *Geology*, *37*(4), 379–382. https://doi.org/10.1130/G25557A.1
Garber, K. L., Finzel, E. S., & Pearson, D. M. (2020). Provenance of synorogenic foreland basin strata in Southwestern Montana requires revision of existing models for Laramide tectonism: North American Cordillera. *Tectonics*, *39*, 26, e2019TC005944. https://doi.org/10.1029/2019TC005944
Garzanti, E. (2019). Petrographic classification of sand and sandstone. *Earth-Science Reviews*, *192*, 545–563. https://doi.org/10.1016/j.earscirev.2018.12.014
Gaschnig, R. M., Macho, A. S., Fayon, A., Schmitz, M., Ware, B. D., Vervoort, J. D., et al. (2017). Intrusive and depositional constraints on the Cretaceous tectonic history of the southern Blue Mountains, eastern Oregon. *Lithosphere*, *9*(2), 265–282. https://doi.org/10.1130/L554.1
Gaschnig, R. M., Vervoort, J. D., Lewis, R. S., & McClelland, W. C. (2010). Migrating magmatism in the northern U.S. Cordillera: In situ U-Pb geochronology of the Idaho batholith. *Contributions to Mineralogy and Petrology*, *159*, 863–883. https://doi.org/10.1007/s00410-009-0459-5
Gehrels, G., Rusmore, M., Woodsworth, G., Crawford, M., Andronicos, C., Hollister, L., et al. (2009). U-Th-Pb geochronology of the Coast Mountains batholith in north-coastal British Columbia: Constraints on age and tectonic evolution. *The Geological Society of America Bulletin*, *121*(9–10), 1341–1361. https://doi.org/10.1130/B26404.1
Gehrels, G. E. (2010). *AgePick*. (Last accessed: March 2020). Retrieved from https://sites.google.com/a/laserchron.org/laserchron/home/
Gehrels, G. E., & Pecha, M. (2014). Detrital zircon U-Pb geochronology and Hf isotope geochemistry of Paleozoic and Triassic passive margin strata of western North America. *Geosphere*, *10*(1), 49–65.
Gehrels, G. E., Valencia, V. A., & Ruiz, J. (2008). Enhanced precision, accuracy, efficiency, and spatial resolution of U-Pb ages by laser ablation-multicollector-inductively coupled plasma-mass spectrometry. *Geochemistry, Geophysics, Geosystems*, *9*, Q03017. https://doi.org/10.1029/2007GC001805
Gentry, A., Yonkee, W. A., Wells, M. L., & Balgord, E. A. (2018). Resolving the history of early fault slip and foreland basin evolution along the Wyoming salient of the Sevier fold-and-thrust belt: Integrating detrital zircon geochronology, provenance modeling, and subsidence analysis. In R. V. Ingersoll, T. F. Lawton, & S. A. Graham (Eds.), Tectonics, Sedimentary Basins, and Provenance: A Celebration of William R. Dickinson's Career (Vol. 540, pp. 509–545). Geological Society of America Special Paper. https://doi.org/10.1130/2018.2540(23)
Ghosh, D. K. (1995). U-Pb geochronology of Jurassic to early Tertiary granitic intrusives from the Nelson-Castlegar area, southeastern British Columbia, Canada. *Canadian Journal of Earth Sciences*, *32*, 1668–1680. https://doi.org/10.1139/e95-132

Gillespie, J. M. (1992). *Tectonic significance of the Jura-Cretaceous strata in the western interior foreland basin of Southern Canada and Northwestern Montana, U.S.* (pp. 150). Laramie, WY: University of Wyoming. Ph.D. thesis.

Gillespie, J. M., & Heller, P. L. (1995). Beginning of foreland subsidence in the Columbian-Sevier belts, southern Canada and northwest Montana. *Geology*, *23*(8), 723–726. https://doi.org/10.1130/0091-7613(1995)023<0723:bofsit>2.3.co;2

Giorgis, S., McClelland, W., Fayon, A., Singer, B. S., & Tikoff, B. (2008). Timing of deformation and exhumation in the western Idaho shear zone, McCall, Idaho. *The Geological Society of America Bulletin*, *120*(9–10), 1119–1133. https://doi.org/10.1130/B26291.1

Giorgis, S., Tikoff, B., & McClelland, W. (2005). Missing Idaho arc: Transpressional modification of the 87Sr/86Sr transition on the western edge of the Idaho batholith. *Geology*, *33*(6), 469–472. https://doi.org/10.1130/G20911.1

Glaister, R. P. (1959). Lower Cretaceous of southern Alberta and adjoining areas. *Bulletin of the American Association of Petroleum Geologists*, *43*(3), 590–640.

Gray, K. D., Isakson, V., Schwartz, D., & Vervoort, J. D. (2019). Orogenic link ~41°N–46°N: Collisional mountain building and basin closure in the Cordillera of western North America. *Geosphere*, *16*, 136–181. https://doi.org/10.1130/GES02074.1

Greig, C. J., Armstrong, R. L., Harakal, J. E., Runkle, D., & der Heyden, P. v. (1992). Geochronometry of the Eagle Plutonic Complex and the Coquihalla area, southwestern British Columbia. *Canadian Journal of Earth Sciences*, *29*, 812–829. https://doi.org/10.1139/e92-068

Gwinn, V. E. (1965). Cretaceous Rocks of the Clark Fork Valley, Central Western Montana. In *16th annual field conference guidebook: Great Falls, Montana* (pp. 34–57). Billings Geological Society, Montana Geological Society.

Hadlari, T., Swindles, G. T., Galloway, J. M., Bell, K. M., Sulphur, K. C., Heaman, L. M., et al. (2015). 1.8 billion years of detrital zircon recycling calibrates a refractory part of Earth's sedimentary cycle. *PloS One*, *10*(12), e0144727. https://doi.org/10.1371/journal.pone.0144727

Haque, Z., Geissman, J. W., DeCelles, P. G., & Carrapa, B. (2020). A magnetostratigraphic age constraint for the proximal synorogenic conglomerates of the Late Cretaceous Cordilleran foreland basin, northeast Utah, USA. *The Geological Society of America Bulletin*. https://doi.org/10.1130/B35768.1

Harris, W. L. (1968). *Stratigraphy and economic geology of the Great Falls – Lewistown Coal Field* (pp. 126). Missoula, MT: University of Montana. M.S. thesis.

Hayes, B. J. R. (1986). Stratigraphy of the basal Cretaceous Lower Mannville Formation, Southern Alberta and North-central Montana. *Bulletin of Canadian Petroleum Geology*, *34*(1), 30–48.

Heller, P. L., Angevine, C. L., Winslow, N. S., & Paola, C. (1988). Two-phase stratigraphic model of foreland-basin sequences. *Geology*, *16*, 501–504. https://doi.org/10.1130/0091-7613(1988)016<0501:tpsmof>2.3.co;2

Heller, P. L., Bowdler, S. S., Chambers, H. P., Coogan, J. C., Hagen, E. S., Shuster, M. W., et al. (1986). Time of initial thrusting in the Sevier orogenic belt, Idaho-Wyoming and Utah. *Geology*, *14*, 388–391. https://doi.org/10.1130/0091-7613(1986)14<388:toitit>2.0.co;2

Heller, P. L., Dueker, K., & McMillan, M. E. (2003). Post-Paleozoic alluvial gravel transport as evidence of continental tilting in the U.S. Cordillera. *The Geological Society of America Bulletin*, *115*(9), 1122–1132. https://doi.org/10.1130/b25219.1

Heller, P. L., & Paola, C. (1989). The paradox of Lower Cretaceous gravels and the initiation of thrusting in the Sevier orogenic belt, United States Western Interior. *The Geological Society of America Bulletin*, *101*, 864–875. https://doi.org/10.1130/0016-7606(1989)101<0864:tpolcg>2.3.co;2

Holm, M. R., James, W. C., & Suttner, L. J. (1977). Comparison of the Peterson and Draney limestones, Idaho and Wyoming, and the calcareous members of the Kootenai Formation, western Montana. In E. L. Heisey (Ed.), *Rocky Mountain thrust belt; Geology and resources: Wyoming geological association 29th annual field conference guidebook* (pp. 259–270). Wyoming Geological Association.

Hopkins, J. C. (1981). Sedimentology of quartzose sandstones of Lower Manville and associated units, Medicine River area, Central Alberta. *Bulletin of Canadian Petroleum Geology*, *29*(1), 12–41.

Hopkins, J. C. (1985). Channel-fill deposits formed by aggradation in deeply scoured, superimposed distributaries of the Lower Kootenai Formation (Cretaceous). *Journal of Sedimentary Petrology*, *55*(1), 42–52.

Horner, S. C., Hubbard, S. M., Martin, H. K., & Hagstrom, C. A. (2019). Reconstructing basin-scale drainage dynamics with regional subsurface mapping and channel-bar scaling, Aptian, Western Canada Foreland Basin. *Sedimentary Geology*, *385*, 26–44. https://doi.org/10.1016/j.sedgeo.2019.03.012

Horton, B. K., Fuentes, F., Boll, A., Starck, D., Ramirez, S. G., & Stockli, D. F. (2016). Andean stratigraphic record of the transition from backarc extension to orogenic shortening: A case study from the northern Neuquén Basin, Argentina. *Journal of South American Earth Sciences*, *71*, 17–40. https://doi.org/10.1016/j.jsames.2016.06.003

Housen, B. A., & Dorsey, R. J. (2005). Paleomagnetism and tectonic significance of Albian and Cenomanian turbidites, Ochoco basin, Mitchell Inlier, central Oregon. *Journal of Geophysical Research*, *110*, B07102. https://doi.org/10.1029/2004JB003458

Hurlow, H. A. (1993). Mid-Cretaceous strike-slip and contractional fault zones in the western Intermontane terrane, Washington, and their relation to the north Cascades-southeastern Coast Belt orogen. *Tectonics*, *12*(5), 1240–1257. https://doi.org/10.1029/93tc01061

Ingersoll, R. V. (2012). Tectonics of sedimentary basins, with revised nomenclature. In C. Busby, & A. Azor Perez (Eds.), *Tectonics of sedimentary basins: Recent advances* (1st ed., pp. 1–42). Blackwell Publishing Ltd.

Ingersoll, R. V., Bullard, T. F., FordGrimm, R. L. J. P., Pickle, J. D., & Sares, S. W. (1984). The effect of grain size on detrital modes: A test of the Gazzi-Dickinson point-counting method. *Journal of Sedimentary Petrology*, *54*(1), 0103–0116. https://doi.org/10.2466/pr0.1984.54.1.129

Irving, E., Wynne, P. J., Thorkelson, D. J., & Schiarizza, P. (1996). Large (1,000 to 4,000 km) northward movements of tectonic domains in the northern Cordillera, 83 to 45 Ma. *Journal of Geophysical Research*, *101*(B8), 17901–17916. https://doi.org/10.1029/96jb01181

James, W. C. (1977). *Origin of nonmarine-marine transitional strata at the top of the Kootenai Formation, southwestern Montana* (pp. 433). Bloomington, IN: Indiana University. Ph.D. thesis.

James, W. C. (1980). Limestone channel storm complex (Lower Cretaceous) Elkhorn Mountains, Montana. *Journal of Sedimentary Petrology*, *50*(2), 447–456.

James, W. C., & Oaks, R. Q. (1977). Petrology of the Kinnikinic Quartzite (Middle Ordovician), East-central Idaho. *Journal of Sedimentary Petrology*, *47*(4), 1491–1511.

Joeckel, R. M., Ludvigson, G. A., Möller, A., Hotton, C. L., Suarez, M. B., Suarez, C. A., et al. (2020). Chronostratigraphy and terrestrial paleoclimatology of Berriasian-Hauterivian strata of the Cedar Mountain Formation, Utah, USA. In M. Wagreich, M. B. Hart, B. Sames, & I. O. Yilmaz (Eds.), Cretaceous Climate Events and Short-Term Sea-Level Changes (Vol. 498, pp. 75–100). Geological Society, London, Special Publications. https://doi.org/10.1144/SP498-2018-133

Jordan, T. E. (1981). Thrust loads and foreland basin evolution, Cretaceous, Western United States. *The American Association of Petroleum Geologists Bulletin*, *65*(12), 2506–2520.

Kauffman, M. E., & Earll, F. N. (1963). Geology of the Garnet-Bearmouth Area, western Montana. In *Montana Bureau of Mines and Geology Memoir 39* (pp. 40). Montana Bureau of Mines and Geology.

Kurz, G. A., Schmitz, M. D., Northrup, C. J., & Vallier, T. L. (2012). U-Pb geochronology and geochemistry of intrusive rocks from the Cougar Creek Complex, Wallowa arc terrane, Blue Mountains Province, Oregon-Idaho. *The Geological Society of America Bulletin*, *124*(3/4), 578–595. https://doi.org/10.1130/B30452.1

LaMaskin, T. A., Vervoort, J. D., Dorsey, R. J., & Wright, J. E. (2011). Early Mesozoic paleogeographic and tectonic evolution of the western United States: Insights from detrital zircon U-Pb geochronology, Blue Mountains Province, northeastern Oregon. *The Geological Society of America Bulletin*, *123*(9–10), 1939–1965. https://doi.org/10.1130/B30260.1

Laskowski, A. K., DeCelles, P. G., & Gehrels, G. E. (2013). Detrital zircon geochronology of Cordilleran retroarc foreland basin strata, western North America. *Tectonics*, *32*, 1027–1048. https://doi.org/10.1002/tect.20065

Lawton, T. F. (2019). Laramide sedimentary basins and sediment-dispersal systems. In A. D. Miall (Ed.), The sedimentary Basins of the United States and Canada (Vol. 2, pp. 529–557). Elsevier. https://doi.org/10.1016/B978-0-444-63895-3.00013-9

Lawton, T. F., Hunt, G. J., & Gehrels, G. E. (2010). Detrital zircon record of thrust belt unroofing in Lower Cretaceous synorogenic conglomerates, central Utah. *Geology*, *38*(5), 463–466. https://doi.org/10.1130/G30684.1

Leary, R. J., Umhoefer, P., Smith, M. E., Smith, T. M., Saylor, J. E., Riggs, N., et al. (2020). Provenance of Pennsylvanian-Permian sedimentary rocks associated with the Ancestral Rocky Mountains orogeny in southwestern Laurentia: Implications for continental-scale Laurentian sediment transport systems. *Lithosphere*, *12*(1), 34. https://doi.org/10.1130/L1115.1

Leckie, D. A., & Smith, D. G. (1992). Regional setting, evolution, and depositional cycles of the Western Canada Foreland Basin. In R. W. Macqueen, & D. A. Leckie (Eds.), *Foreland basins and fold belts: AAPG Memoir 55* (pp. 9–46). Tulsa, OK: The American Association of Petroleum Geologists.

Leier, A. L., & Gehrels, G. E. (2011). Continental-scale detrital zircon provenance signatures in Lower Cretaceous strata, western North America. *Geology*, *39*(4), 399–402. https://doi.org/10.1130/G31762.1

Lewis, R. S., Vervoort, J. D., Burmester, R. F., & Oswald, P. J. (2010). Detrital zircon analysis of Mesoproterozoic and Neoproterozoic metasedimentary rocks of north-central Idaho: Implications for development of the Belt-Purcell basin. *Canadian Journal of Earth Sciences*, *47*(11), 1383–1404. https://doi.org/10.1139/E10-049

Link, P. K., Fanning, C. M., Lund, K. I., & Aleinikoff, J. N. (2007). Detrital-zircon populations and provenance of Mesoproterozoic Strata of east-central Idaho, U.S.A. Correlation with Belt Supergroup of southwest Montana. In P. K. Link & R. S. Lewis (Eds.), Proterozoic Geology of Western North America and Siberia (Vol. 86, pp. 101–128). Tulsa, OK: SEPM (Society for Sedimentary Geology).

Link, P. K., Mahon, R. C., Beranek, L. P., Campbell-Stone, E. A., & Lynds, R. (2014). Detrital zircon provenance of Pennsylvanian to Permian sandstones from the Wyoming craton and Wood River Basin, Idaho, U.S.A. *Rocky Mountain Geology*, *49*(2), 115–136. https://doi.org/10.2113/gsrocky.49.2.115

Link, P. K., Stewart, E. D., Steel, T., Sherwin, J., Hess, L. T., & McDonald, C. (2016). Detrital zircons in the Mesoproterozoic upper Belt Supergroup in the Pioneer, Beaverhead, and Lemhi Ranges, Montana and Idaho: The Big White arc. In J. S. MacLean, & J. W. Sears (Eds.), *Belt Basin: Window to Mesoproterozoic Earth, Geological Society of America Special Paper 522* (pp. 163–183). The Geological Society of America. https://doi.org/10.1130/2016.2522(07)

Link, P. K., Todt, M. K., Pearson, D. M., & Thomas, R. C. (2017). 500–490 Ma detrital zircons in Upper Cambrian Worm Creek and correlative sandstones, Idaho, Montana, and Wyoming: Magmatism and tectonism within the passive margin. *Lithosphere*, *9*(6), 910–926. https://doi.org/10.1130/L671.1

Link, P. K., Warren, I., Preacher, J. M., & Skipp, B. (1996). Stratigraphic Analysis and Interpretation of the Mississippian Copper Basin Group, McGowan Creek Formation, and White Knob Limestone, South-Central Idaho. In M. W. Longman, & D. M. Sonnenfeld (Eds.), *Paleozoic systems of the Rocky Mountain Region* (pp. 117–144). Rocky Mountain Section, SEPM (Society for Sedimentary Geology).

Lonn, J. D., Burmester, R. F., Lewis, R. S., & McFaddan, M. D. (2016). Giant folds and complex faults in Mesoproterozoic Lemhi strata of the Belt Supergroup, northern Beaverhead Mountains, Montana and Idaho. In J. S. MacLean, & J. W. Sears (Eds.), *Belt Basin: Window to Mesoproterozoic Earth, Geological Society of America Special Paper 522* (pp. 139–162). The Geological Society of America. https://doi.org/10.1130/2016.2522(06)

Lund, K., Aleinikoff, J. N., Kunk, M. J., Unruh, D. M., Zeihen, G. D., Hodges, W. C., et al. (2002). SHRIMP U-Pb and $^{40}Ar/^{39}Ar$ age constraints for relating plutonism and mineralization in the Boulder Batholith Region, Montana. *Economic Geology*, *97*, 241–267. https://doi.org/10.2113/gsecongeo.97.2.241

Lund, K. L., & Snee, L. W. (1988). Metamorphism, structural development, and age of the continent-island arc juncture in west-central Idaho. In W. G. Ernst (Ed.), *Metamorphism and crustal evolution of the western United States: Ruby Volume VII* (pp. 296–331). Englewood Cliffs, NJ: Prentice-Hall.

Lund, K., McAleer, R. J., Aleinikoff, J. N., Cosca, M. A., & Kunk, M. J. (2018). Two-event lode-ore deposition at Butte, USA: $^{40}Ar/^{39}Ar$ and U-Pb documentation of Ag-Au-polymetallic lodes overprinted by younger stockwork Cu-Mo ores and penecontemporaneous Cu lodes. *Ore Geology Reviews*, *102*, 666–700. https://doi.org/10.1016/j.oregeorev.2018.05.018

Ma, C., Bergeron, P., Foster, D. A., Dutrow, B. L., Mueller, P. A., & Allen, C. (2016). Detrital-zircon geochronology of the Sawtooth metamorphic complex, Idaho: Evidence for metamorphosed lower Paleozoic shelf strata within the Idaho batholith. *Geosphere*, *12*(4), 1136–1153. https://doi.org/10.1130/GES01201.1

Mann, J. A. (1954). *Geology of part of the gravelly range Montana Yellowstone-Bighorn research project contribution 190* (pp. 92). Yellowstone-Bighorn Research Association.

Matthews, W., Guest, B., & Madronich, L. (2018). Latest Neoproterozoic to Cambrian detrital zircon facies of western Laurentia. *Geosphere*, *14*(1), 243–264. https://doi.org/10.1130/GES01544.1

May, S. R., Gray, G. G., Summa, L. L., Stewart, N. R., Gehrels, G. E., & Pecha, M. E. (2013). Detrital zircon geochronology from the Bighorn Basin, Wyoming, USA: Implications for tectonostratigraphic evolution and paleogeography. *The Geological Society of America Bulletin*, *125*(9–10), 1403–1422. https://doi.org/10.1130/b30824.1

McClelland, W. C., Gehrels, G. E., & Saleeby, J. B. (1992). Upper Jurassic-Lower Cretaceous basinal strata along the Cordilleran margin: Implications for the accretionary history of the Alexander-Wrangellia-Peninsular terrane. *Tectonics*, *11*(4), 823–835. https://doi.org/10.1029/92tc00241

McClelland, W. C., & Oldow, J. S. (2007). Late Cretaceous truncation of the western Idaho shear zone in the central North American Cordillera. *Geology*, *35*(8), 723–726. https://doi.org/10.1130/G23623A.1

McClelland, W. C., Tikoff, B., & Manduca, C. A. (2000). Two-phase evolution of accretionary margins: Examples from the North American Cordillera. *Tectonophysics*, *326*, 37–55. https://doi.org/10.1016/s0040-1951(00)00145-1

Miall, A. D. (2009). Initiation of the Western Interior foreland basin. *Geology*, *37*(4), 383–384. https://doi.org/10.1130/focus042009.1

Monger, J. W. H., Price, R. A., & Tempelman-Kluit, D. J. (1982). Tectonic accretion and the origin of the two major metamorphic and plutonic welts in the Canadian Cordillera. *Geology*, *10*, 70–75. https://doi.org/10.1130/0091-7613(1982)10<70:taatoo>2.0.co;2

Montoya, L. M. (2019). *Investigation of structural style within the Sevier fold-thrust belt along the southwestern boundary of the Lemhi Arch, central Idaho* (pp. 80). Pocatello, ID: Idaho State University. M.S. thesis, 4 Plates.
Mudge, M. R. (1972). Pre-quaternary rocks in the Sun River Canyon area, northwestern Montana. In *U.S. Geological Survey Professional Paper 663-A* (pp. 142). United States Geological Survey.
Mudge, M. R., & Rice, D. D. (1982). Lower Cretaceous Mount Pablo Formation, northwestern Montana. In *U.S. Geological Survey Bulletin 1502-D* (pp. 19). United States Geological Survey.
Nilsen, T. R. (1977). Paleogeography of Mississippian turbidites in south-central Idaho. In *Paleozoic paleogeography of the Western United States: Pacific Section. Society of Economic Paleontologists and Mineralogists Paleogeography Symposium 1* (pp. 275–299), SEPM (Society for Sedimentary Geology).
Oaks, R. Q., Jr., James, W. C., Francis, G. G., & Schulingkamp, W. J., II. (1977). Summary of Middle Ordovician stratigraphy and tectonics, northern Utah, southern and central Idaho. In *29th annual field conference guidebook: Rocky mountain thrust belt geology and resources* (pp. 101–118). Wyoming Geological Association.
Pană, D. I., Poulton, T. P., & DuFrane, S. A. (2019). U-Pb detrital zircon dating supports Early Jurassic initiation of the Cordilleran foreland basin in southwestern Canada. *The Geological Society of America Bulletin*, *131*(1–2), 318–334. https://doi.org/10.1130/B31862.1
Peck, R. E. (1941). Lower Cretaceous Rocky Mountain nonmarine microfossils. *Journal of Paleontology*, *15*(3), 285–304.
Peck, R. E. (1951). Nonmarine ostracodes – the subfamily Cyprideinae in the Rocky Mountain area. *Journal of Paleontology*, *25*(3), 307–320.
Perry, W. J., Jr., Wardlaw, B. R., Bostick, N. H., & Maughan, E. K. (1983). Structure, burial history, and petroleum potential of frontal thrust belt and adjacent foreland, southwest Montana. *AAPG Bulletin*, *67*, 725–743.
Price, R. A. (1981). The Cordilleran foreland thrust and fold belt in the southern Canadian Rocky Mountains. In K. R. McClay, & N. J. Price (Eds.), *Thrust and nappe tectonics, The Geological Society of London, Special Publication 9* (pp. 427–448), The Geological Society of London.
Pullen, A., Ibáñez-Mejia, M., Gehrels, G. E., Giesler, D., & Pecha, M. (2018). Optimization of a laser ablation-single collector-inductively coupled plasma-mass spectrometer (Thermo Element2) for accurate, precise, and efficient Zircon U-Th-Pb geochronology. *Geochemistry, Geophysics, Geosystems*, *19*, 3689–3705. https://doi.org/10.1029/2018GC007889
Quinn, G. M., Hubbard, S. M., Putnam, P. E., Matthews, W. A., Daniels, B. G., & Guest, B. (2018). A Late Jurassic to Early Cretaceous record of orogenic wedge evolution in the Western Interior basin, USA and Canada. *Geosphere*, *14*(3), 1187–1206. https://doi.org/10.1130/GES01606.1
Quinn, G. M., Hubbard, S. M., van Drecht, R., Guest, B., Matthews, W. A., & Hadlari, T. (2016). Record of orogenic cyclicity in the Alberta foreland basin, Canadian Cordillera. *Lithosphere*, *8*(3), 317–332. https://doi.org/10.1130/L531.1
Raines, M. K., Hubbard, S. M., Kukulski, R. B., Leier, A. L., & Gehrels, G. E. (2013). Sediment dispersal in an evolving foreland: Detrital zircon geochronology from Upper Jurassic and lowermost Cretaceous strata, Alberta Basin, Canada. *The Geological Society of America Bulletin*, *125*(5–6), 741–755. https://doi.org/10.1130/B30671.1
Rapson, J. E. (1964). Lithology and petrography of transitional Jurassic-Cretaceous clastic rocks, southern Rocky Mountains. *Bulletin of Canadian Petroleum Geology*, *12*, 556–586.Field Conference Guidebook Issue.
Rapson, J. E. (1965). Petrography and derivation of Jurassic-Cretaceous clastic rocks, southern Rocky Mountains, Canada. *Bulletin of the American Association of Petroleum Geologists*, *49*(9), 1426–1452.
Reid, C. R. (2015). *Incised valley-fill system development and stratigraphic analysis of the Lower Cretaceous Kootenai Formation, Northwest Montana* (pp. 142). Bozeman, MT: Montana State University. M.S. thesis.
Roberts, A. E. (1972). Cretaceous and early Tertiary depositional and tectonic history of the Livingston area, Southwestern Montana. In *United States Geological Survey Professional Paper 526-C* (pp. 120), Washington D.C.: United States Geological Survey.
Rodgers, D. W., Link, P. K., & Huerta, A. D. (1995). Structural framework of mineral deposits hosted by Paleozoic rocks in the northeastern part of the Hailey 1 × 2 quadrangle, south-central Idaho. In R. G. Worl, P. K. Link, G. R. Winkler, & K. M. Johnson (Eds.), *Geology and mineral resources of the Hailey and Idaho Falls quadrangles* (Vol. *2064*, pp. E1–E27). U.S. Geological Survey Bulletin. https://doi.org/10.3133/b2064AR
Ronemus, C. B., Orme, D. A., Campbell, S., Black, S. R., & Cook, J. (2020). Mesoproterozoic-Early Cretaceous provenance and paleogeographic evolution of the Northern Rocky Mountains: Insights from the detrital zircon record of the Bridger range, Montana, USA. *The Geological Society of America Bulletin*, *133*, 777–801. https://doi.org/10.1130/B35628.1
Ross, C. P. (1934). Correlation and interpretation of Paleozoic stratigraphy in south-central Idaho. *The Geological Society of America Bulletin*, *45*(5), 937–1000. https://doi.org/10.1130/gsab-45-937
Ross, G. M., & Parrish, R. R. (1991). Detrital zircon geochronology of metasedimentary rocks in the southern Omineca Belt, Canadian Cordillera. *Canadian Journal of Earth Sciences*, *28*, 1254–1270. https://doi.org/10.1139/e91-112
Royse, F., Jr. (1993). Case of the phantom foredeep: Early Cretaceous in west-central Utah. *Geology*, *21*, 133–136. https://doi.org/10.1130/0091-7613(1993)021<0133:cotpfe>2.3.co;2
Ruppel, E. T., & Lopez, D. A. (1984). The Thrust Belt in Southwest Montana and East-Central Idaho. In *United States Geological Survey Professional Paper 1278* (pp. 41), Washington D.C.: United States Geological Survey.
Ryder, R. T., & Scholten, R. (1973). Syntectonic Conglomerates in Southwestern Montana: Their nature, origin, and tectonic significance. *The Geological Society of America Bulletin*, *84*, 773–796. https://doi.org/10.1130/0016-7606(1973)84<773:scismt>2.0.co;2
Saylor, J. E., Jordan, J. C., Sundell, K. E., Wang, X., Wang, S., & Deng, T. (2017). Topographic growth of the Jishi Shan and its impact on basin and hydrology evolution, NE Tibetan Plateau. *Basin Research*, 1–20. https://doi.org/10.1111/bre.12264
Saylor, J. E., & Sundell, K. E. (2016). Quantifying comparison of large detrital geochronology data sets. *Geosphere*, *12*(1), 203–220. https://doi.org/10.1130/GES01237.1
Schmidt, C. J., & Garihan, J. M. (1983). Laramide tectonic development of the Rocky Mountain foreland of southwestern Montana. In J. D. Lowell (Ed.), *Rocky Mountain foreland basins and uplifts* (pp. 271–294). Denver, CO: Rocky Mountain Association of Geologists.
Schmidt, C. J., & O'Neill, J. M. (1983). Structural evolution of the southwest Montana transverse zone. In R. W. Powers (Eds.), *Geologic studies of the Cordilleran thrust belt – 1982* (pp. 193–218). Denver, CO: Rocky Mountain Association of Geologists.
Schmidt, C. J., O'Neill, J. M., & Brandon, W. C. (1988). Influence of Rocky Mountain foreland uplifts on the development of the frontal fold and thrust belt, southwestern Montana. In C. J. Schmidt, & W. J. Perry Jr. (Eds.), Interaction of the Rocky Mountain foreland and the Cordilleran thrust belt (Vol. 171, pp. 171–201). Denver, CO: Geological Society of America MemoirGeological Society of America.
Schmidt, K. L., Lewis, R. S., Vervoort, J. D., Stetson-Lee, T. A., Michels, Z. D., & Tikoff, B. (2017). Tectonic evolution of the Syringa embayment in the central North American Cordilleran accretionary boundary. *Lithosphere*, *9*(2), 184–204. https://doi.org/10.1130/L545.1
Schwartz, J. J., Johnson, K., Miranda, E. A., & Wooden, J. L. (2011). The generation of high Sr/Y plutons following Late Jurassic arc-arc collision, Blue Mountains province, NE Oregon. *Lithos*, *126*, 22–41. https://doi.org/10.1016/j.lithos.2011.05.005

Schwartz, J. J., Johnson, K., Mueller, P., Valley, J., Strickland, A., & Wooden, J. L. (2014). Time scales and processes of Cordilleran batholith construction and high-Sr/Y magmatic pulses: Evidence from the Bald Mountain batholith, northeastern Oregon. *Geosphere*, *10*(6), 1456–1481. https://doi.org/10.1130/GES01033.1

Schwartz, J. J., Snoke, A. W., Cordey, F., Johnson, K., Frost, C. D., Barnes, C. G., et al. (2011). Late Jurassic magmatism, metamorphism, and deformation in the Blue Mountains Province, northeast Oregon. *The Geological Society of America Bulletin*, *123*(9–10), 2083–2111. https://doi.org/10.1130/B30327.1

Schwartz, J. J., Snoke, A. W., Frost, C. D., Barnes, C. G., Gromet, L. P., & Johnson, K. (2010). Analysis of the Wallowa–Baker terrane boundary: Implications for tectonic accretion in the Blue Mountains province, northeastern Oregon. *The Geological Society of America Bulletin*, *122*(3–4), 517–536. https://doi.org/10.1130/B26493.1

Schwartz, R. K. (1972). *Stratigraphic and petrographic analysis of the Lower Cretaceous Blackleaf Formation, southwestern Montana* (pp. 268). Bloomington, IN: Indiana University. Ph.D. thesis.

Schwartz, R. K. (1983). Broken Early Cretaceous Foreland Basin in southwestern Montana: Sedimentation related to tectonism. In R. B. Powers (Ed.), Geologic Studies of the Cordilleran Thrust Belt (Vol. 1, pp. 159–184). Denver, CO: Rocky Mountain Association of Geologists.

Schwartz, R. K., & DeCelles, P. G. (1988). Cordilleran Foreland Basin evolution in response to interactive Cretaceous thrusting and foreland partitioning, southwestern Montana. In C. J. Schmidt, & W. J. Perry Jr. (Eds.), Interaction of the Rocky Mountain foreland and the Cordilleran thrust belt, Geological Society of America Memoir (Vol. 171, pp. 489–513). Denver, CO: Geological Society of America.

Schwartz, R. K., & Vuke, S. (2019). Estuarine deposits in the Kootenai Formation as evidence of an Early Cretaceous (pre-Albian) marine advance into western Montana and relationship to Cordilleran foreland basin evolution. In *Montana Bureau of Mines and Geology, Memoir 69* (pp. 88), Montana Bureau of Mines and Geology.

Schwartz, T. M., Schwartz, R. K., & Weislogel, A. L. (2019). Orogenic recycling of d zircons characterizes age distributions of North American Cordilleran Strata. *Tectonics*, *38*. https://doi.org/10.1029/2019TC005810

Sevigny, J. H., & Parrish, R. R. (1993). Age and origin of Late Jurassic and Paleocene granitoids, Nelson Batholith, southern British Columbia. *Canadian Journal of Earth Sciences*, *30*, 2305–2314. https://doi.org/10.1139/e93-200

Singh, C. (1964). Microflora of the lower Cretaceous Mannville Group, east-central Alberta. In *Alberta Research Council Bulletin 15* (pp. 238).

Skipp, B. (1988). Cordilleran thrust belt and faulted foreland in the Beaverhead Mountains, Idaho and Montana. In C. J. Schmidt, & W. J. Perry Jr. (Eds.), Interaction of the Rocky Mountain foreland and the Cordilleran thrust belt, Geological Society of America Memoir (Vol. 171, pp. 237–266). Denver, CO: Geological Society of America.

Skipp, B., & Hait, M. H., Jr. (1977). Allochthons along the northeast margin of the Snake River Plain, Idaho. In E. L. Heisey (Ed.), *Rocky Mountain thrust belt; Geology and resources: Wyoming geological association 29th annual field conference guidebook* (pp. 499–515), Wyoming Geological Association.

Spencer, C. J., Kirkland, C. L., & Taylor, R. J. M. (2016). Strategies toward statistically robust interpretations of in situ U-Pb zircon geochronology. *Geoscience Frontiers*, *7*, 581–589. https://doi.org/10.1016/j.gsf.2015.11.006

Stacey, J. S., & Kramers, J. D. (1975). Approximation of terrestrial lead isotope evolution by a two-stage model. *Earth and Planetary Science Letters*, *26*, 207–221. https://doi.org/10.1016/0012-821x(75)90088-6

Stanton, T. (1903). A new fresh-water molluscan faunule from the Cretaceous of Montana. *Proceedings of the American Philosophical Society*, *42*(173), 188–199.

Stewart, E. D., Link, P. K., Fanning, C. M., Frost, C. D., & McCurry, M. (2010). Paleogeographic implications of non-North American sediment in the Mesoproterozoic upper Belt Supergroup and Lemhi Group, Idaho and Montana, USA. *Geology*, *38*, 927–930. https://doi.org/10.1130/G31194.1

Sundell, K. E., Gehrels, G. E., & Pecha, M. E. (2020). Rapid U-Pb Geochronology by Laser Ablation Multi-collector ICP-MS. *In Geostandards and geoanalytical research*, *45*(1), 35–57.

Sundell, K. E., & Saylor, J. E. (2017). Unmixing detrital geochronology age distributions. *Geochemistry, Geophysics, Geosystems*, *18*, 2872–2886. https://doi.org/10.1002/2016GC006774

Surpless, K. D., Sickmann, Z. T., & Koplitz, T. A. (2014). East-derived strata in the Methow basin record rapid mid-Cretaceous uplift of the southern Coast Mountains batholith. *Canadian Journal of Earth Sciences*, *51*, 339–357. https://doi.org/10.1139/cjes-2013-0144

Suttner, L. J. (1969). Stratigraphic and petrographic analysis of Upper Jurassic-Lower Cretaceous Morrison and Kootenai Formations, Southwest Montana. *AAPG Bulletin*, *53*(7), 1391–1410.

Suttner, L. J., Schwartz, R. K., & James, W. C. (1981). Late Mesozoic to Early Cenozoic foreland sedimentation in southwest Montana. In *Montana Geological Society Field Conference and Symposium Guidebook to southwest Montana* (pp. 93–103). Montana Geological Society.

Thomas, W. A. (2011). Detrital-zircon geochronology and sedimentary provenance. *Lithosphere*, *3*(4), 304–308. https://doi.org/10.1130/RF.L001.1

Tysdal, R. G. (2002). Structural geology of western part of Lemhi Range, east-central Idaho. In *U.S. Geological Survey Professional Paper, 1659*. United States Geological Survey. https://10.3133/pp1659

Umpleby, J. B., Westgate, L. G., & Ross, C. P. (1930). Geology and ore deposits of the Wood River region, Idaho. In *The Geological Society of America Bulletin 814* (pp. 250).

Unruh, D. M., Lund, K., Kuntz, M. A., & Snee, L. W. (2008). *Uranium-lead zircon ages and Sr, Nd, and Pb isotope geochemistry of selected plutonic rocks from western Idaho* (pp. 37). U.S. Geological Survey Open-File Report 2008-1142.

van der Velon, A. J., & Cook, F. A. (1996). Structure and tectonic development of the southern Rocky Mountain trench. *Tectonics*, *15*(3), 517–544. https://doi.org/10.1029/95TC03288

Vermeesch, P. (2013). Multi-sample comparison of detrital age distributions. *Chemical Geology*, *341*, 140–146. http://dx.doi.org/10.1016/j.chemgeo.2013.01.010

Vuke, S. M. (1982). *Depositional environments of the Cretaceous Thermopolis, Muddy and Mowry formations, southern Madison and Gallatin Ranges* (pp. 141). Missoula, MT: University of Montana. M.S. thesis.

Vuke, S. M. (1984). Depositional environments of the Early Cretaceous Western Interior Seaway in southwestern Montana and the northern United States. In D. F. Stott, & D. J. Glass (Eds.), *The Mesozoic of Middle North America, Canadian Society of Petroleum Geologists Memoir 9* (pp. 127–144).

Vuke, S. M. (2000). Geologic map of the Great Falls south 30' × 60' Quadrangle, central Montana. In *Montana Bureau of Mines and Geology* (pp. 18). Open File Report MBMG 407, Montana Bureau of Mines and Geology.

Vuke, S. M., Porter, K. W., Lonn, J. D., & Lopez, D. A. (2007). Geologic map of Montana. In *Montana Bureau of Mines and Geology*, Geological Map, 62. 1:500,000 scale.

Walker, T. F. (1974). *Stratigraphy and depositional environments of the Morrison and Kootenai formations in the Great Falls area, central Montana* (pp. 195). Missoula, MT: University of Montana. Ph.D. thesis.

Ware, B. D. (2013). *Age, provenance, and structure of the Weatherby Formation, eastern Izee sub-basin, Blue Mountains province, Oregon and Idaho* (pp. 249). Boise, ID: Boise State University. M.S. thesis.

Webster, E. R., Pattison, D., & DuFrane, S. A. (2017). Geochronological constraints on magmatism and polyphase deformation and metamorphism in the southern Omineca Belt, British Columbia. *Canadian Journal of Earth Sciences*, *54*, 529–549. https://doi.org/10.1139/cjes-2016-0126

Wernicke, B., & Klepacki, D. W. (1988). Escape hypothesis for the Stikine block. *Geology*, *16*, 461–464. https://doi.org/10.1130/0091-7613(1988)016<0461:ehftsb>2.3.co;2

Whitmeyer, S., & Karlstrom, K. E. (2007). Tectonic model for the Proterozoic growth of North America. *Geosphere*, *3*(4), 220–259. https://doi.org/10.1130/GES00055.1

Wright, J. E., & Wyld, S. J. (2007). Alternative tectonic model for Late Jurasssic through Early Cretaceous evolution of the Great Valley Group, California. In M. Cloos, W. D. Carlson, M. C. Gilbert, J. G. Liou, & S. S. Sorensen (Eds.), *Covergent margin terranes and associated regions: A tribute to W.G. Ernst, Geological Society of America, Special Paper 419* (pp. 81–95), The Geological Society of America. https://doi.org/10.1130/2007.2419(04)

Wyld, S. J., Umhoefer, P. J., & Wright, J. E. (2006). Reconstructing northern Cordilleran terranes along known Cretaceous and Cenozoic strike-slip faults: Implications for the Baja British Columbia hypothesis and other models. In J. W. Haggart, R. J. Enkin, & J. W. H. Monger (Eds.), *Paleogeography of the North American Cordillera: Evidence for and against large-scale displacements: Geological Association of Canada, Special Paper, 46* (pp. 277–298), Geological Association of Canada.

Yen, T. C. (1949). Review of the Lower Cretaceous fresh-water molluscan faunas of North America. *Journal of Paleontology*, *23*, 465–470.

Yen, T. C. (1951). Fresh-water mollusks of Cretaceous age from Montana and Wyoming. In *United States Geological Survey Professional Paper 233-A* (pp. 1–20), United States Geological Survey.

Yonkee, W. A., & Weil, A. B. (2015). Tectonic evolution of the Sevier and Laramide belts within the North American Cordillera orogenic system. *Earth-Science Reviews*, *150*, 531–593. https://doi.org/10.1016/j.earscirev.2015.08.001

Zaleha, M. J. (2006). Sevier orogenesis and nonmarine basin filling: Implications of new stratigraphic correlations of Lower Cretaceous strata throughout Wyoming, USA. *The Geological Society of America Bulletin*, *118*(7/8), 886–896. https://doi.org/10.1130/B25715.1